

# Development of an Eco-Friendly, Cost-Effective Biogrout for Concrete Crack Repair

**Final Report**  
**September 2016**

---

**Sponsored by**  
Midwest Transportation Center  
U.S. Department of Transportation  
Office of the Assistant Secretary for  
Research and Technology



## **About MTC**

The Midwest Transportation Center (MTC) is a regional University Transportation Center (UTC) sponsored by the U.S. Department of Transportation Office of the Assistant Secretary for Research and Technology (USDOT/OST-R). The mission of the UTC program is to advance U.S. technology and expertise in the many disciplines comprising transportation through the mechanisms of education, research, and technology transfer at university-based centers of excellence. Iowa State University, through its Institute for Transportation (InTrans), is the MTC lead institution.

## **About InTrans**

The mission of the Institute for Transportation (InTrans) at Iowa State University is to develop and implement innovative methods, materials, and technologies for improving transportation efficiency, safety, reliability, and sustainability while improving the learning environment of students, faculty, and staff in transportation-related fields.

## **ISU Non-Discrimination Statement**

Iowa State University does not discriminate on the basis of race, color, age, ethnicity, religion, national origin, pregnancy, sexual orientation, gender identity, genetic information, sex, marital status, disability, or status as a U.S. veteran. Inquiries regarding non-discrimination policies may be directed to Office of Equal Opportunity, Title IX/ADA Coordinator, and Affirmative Action Officer, 3350 Beardshear Hall, Ames, Iowa 50011, 515-294-7612, email [eoffice@iastate.edu](mailto:eoffice@iastate.edu).

## **Notice**

The contents of this report reflect the views of the authors, who are responsible for the facts and the accuracy of the information presented herein. The opinions, findings and conclusions expressed in this publication are those of the authors and not necessarily those of the sponsors.

This document is disseminated under the sponsorship of the U.S. DOT UTC program in the interest of information exchange. The U.S. Government assumes no liability for the use of the information contained in this document. This report does not constitute a standard, specification, or regulation.

The U.S. Government does not endorse products or manufacturers. If trademarks or manufacturers' names appear in this report, it is only because they are considered essential to the objective of the document.

## **Quality Assurance Statement**

The Federal Highway Administration (FHWA) provides high-quality information to serve Government, industry, and the public in a manner that promotes public understanding. Standards and policies are used to ensure and maximize the quality, objectivity, utility, and integrity of its information. The FHWA periodically reviews quality issues and adjusts its programs and processes to ensure continuous quality improvement.

**Technical Report Documentation Page**

<b>1. Report No.</b>	<b>2. Government Accession No.</b>	<b>3. Recipient's Catalog No.</b>	
<b>4. Title and Subtitle</b> Development of an Eco-Friendly, Cost-Effective BiogROUT for Concrete Crack Repair		<b>5. Report Date</b> September 2016	
		<b>6. Performing Organization Code</b>	
<b>7. Author(s)</b> Kejin Wang, Zhiyou Wen, and Sungyu Choi		<b>8. Performing Organization Report No.</b>	
<b>9. Performing Organization Name and Address</b> Institute for Transportation Iowa State University 2711 South Loop Drive, Suite 4700 Ames, IA 50010-8664		<b>10. Work Unit No. (TRAIS)</b>	
		<b>11. Contract or Grant No.</b> Part of DTRT13-G-UTC37	
<b>12. Sponsoring Organization Name and Address</b> Midwest Transportation Center 2711 S. Loop Drive, Suite 4700 Ames, IA 50010-8664		<b>13. Type of Report and Period Covered</b> Final Report	
		<b>14. Sponsoring Agency Code</b>	
<b>15. Supplementary Notes</b> Visit <a href="http://www.intrans.iastate.edu">www.intrans.iastate.edu</a> for color pdfs of this and other research reports.			
<b>16. Abstract</b> <p>Typical concrete crack repair uses chemical sealants or surface treatment agents, which are often expensive and harmful to environment. The goal of this study was to develop an eco-friendly, cost-effective biogROUT for concrete crack repair.</p> <p>A biocement was developed using microbiologically induced calcium carbonate precipitation (MICP) technology. A biomass of urease-producing bacteria (UPB) (e.g., <i>Bacillus sphaericus</i>), urea, and a soluble calcium solution were used for the MICP process. The study included two major parts. The first part was to develop a new soluble calcium solution for MICP by dissolving a limestone powder, a by-product from a limestone quarry, into an acetic acid-rich stage fraction 5 (SF5) solution derived from biomass pyrolysis and a fractionation system. The second part was to study mortar crack repair using MICP technology.</p> <p>The results indicated that the properties of the new soluble calcium solution for MICP could be optimized from the study of different limestone powder-to-SF5 ratios, potential of hydrogen (pH) values of the obtained solutions, and procedures for applying the UPB and media (urea/calcium solutions) for calcium carbonate (CaCO<sub>3</sub>) precipitation (i.e., MICP treatment). Using such a soluble calcium solution as a replacement for calcium chloride (CaCl<sub>2</sub>) in the MICP process produced desirable CaCO<sub>3</sub> precipitation. The properties of the sand samples cemented using the limestone-SF5 calcium solution were comparable to those of the sand samples reported in previous studies, where CaCl<sub>2</sub> was commonly used as a soluble calcium solution. Cracks in mortar samples repaired using the MICP technology gradually healed with an increasing number of MICP treatment cycles. The samples treated with MICP had a significant reduction in water permeability. While water-treated samples were too weak to test, the MICP-treated samples had splitting tensile strength (TS) ranging from 32 to 386 kPa after 21 treatment cycles. For the samples having an initial average crack width of &gt;0.52 mm, the TS clearly increased with the CaCO<sub>3</sub> content resulting from the MICP treatment. A scanning electron microscope (SEM) study suggested that there were two different forms of CaCO<sub>3</sub> on the crack surface of cracked mortar samples: one was vaterite and the other calcite. The CaCO<sub>3</sub> crystals had a size ranging from 5 to 20 μm, and they formed a porous matrix that filled in the mortar cracks.</p>			
<b>17. Key Words</b> biocement utilization—biogROUT—concrete crack repair—concrete pavement patches—high-performance mortar—limestone fines—rapid repair		<b>18. Distribution Statement</b> No restrictions.	
<b>19. Security Classification (of this report)</b> Unclassified.	<b>20. Security Classification (of this page)</b> Unclassified.	<b>21. No. of Pages</b> 57	<b>22. Price</b> NA



# **DEVELOPMENT OF AN ECO-FRIENDLY, COST-EFFECTIVE BIOGROUT FOR CONCRETE CRACK REPAIR**

**Final Report**  
**September 2016**

**Principal Investigator**  
Kejin Wang, Professor  
Civil, Construction, and Environmental Engineering, Iowa State University

**Co-Principal Investigator**  
Zhiyou Wen, Associate Professor  
Food Science, Iowa State University

**Research Assistants**  
Sungyu Choi

**Authors**  
Kejin Wang, Zhiyou Wen, and Sungyu Choi

Sponsored by  
Midwest Transportation Center and  
U.S. Department of Transportation  
Office of the Assistant Secretary for Research and Technology

A report from  
**Institute for Transportation**  
**Iowa State University**  
2711 South Loop Drive, Suite 4700  
Ames, IA 50010-8664  
Phone: 515-294-8103 / Fax: 515-294-0467  
[www.intrans.iastate.edu](http://www.intrans.iastate.edu)



## TABLE OF CONTENTS

ACKNOWLEDGMENTS .....	ix
EXECUTIVE SUMMARY .....	xi
1 INTRODUCTION .....	1
1.1 Background.....	1
1.2 Objectives .....	1
2 LITERATURE REVIEW .....	2
2.1 Microbiologically Induced Calcium Carbonate Precipitation .....	2
2.2 Applications of MICP in Earth Materials .....	3
2.3 Applications of MICP in Concrete Materials .....	6
3 RESEARCH APPROACH AND SCOPE .....	10
4 BIOGROUT DEVELOPMENT .....	11
4.1 Preparing Materials and Solutions.....	11
4.2 MICP Tests and Precipitated CaCO <sub>3</sub> .....	13
4.3 MICP Test for Sand Cementation.....	14
4.4 Evaluation of Properties of the Biocemented Sand .....	16
4.5 Summary.....	20
5 MORTAR CRACK REPAIR .....	22
5.1 Materials and Sample Preparation .....	22
5.2 Test and Methods.....	28
5.3 Results and Discussion .....	29
5.4 Summary.....	38
6 CONCLUSIONS AND RECOMMENDATIONS .....	40
REFERENCES .....	43

## LIST OF FIGURES

Figure 1. Concept of biocementation (left) and sample of biocemented sand (right) from MICP .....	2
Figure 2. Effect of $\text{CaCO}_3$ content on the UCS of MICP-treated sand .....	6
Figure 3. Precipitated materials observed during MICP tests.....	14
Figure 4. XRD result of the precipitated material observed from the MICP using the calcium solution made from limestone powder and SF5 .....	14
Figure 5. Sketch of MICP test setup (left) and actual (right).....	15
Figure 6. Cemented sand after MICP treatment .....	16
Figure 7. Effect of $\text{CaCO}_3$ content on permeability of biocemented sand.....	17
Figure 8. Strain-stress relationships of biocemented sand showing UCS (left) and TS (right) .....	18
Figure 9. Physio-mechanical properties of biocemented sand showing UCS (top), TS (middle), and UCS/TS ratio (bottom) .....	19
Figure 10. Biocemented sand with two sand particles connected by $\text{CaCO}_3$ (left) and cubic shaped $\text{CaCO}_3$ (right) under a SEM .....	20
Figure 11. Preparation of cylinder mold for mortar sample casting: metal wires attached on half rods (top), half rods in cylinder mold (left), and half rods in cast mortar sample (right) .....	23
Figure 12. Making a crack in a mortar sample by splitting mortar using a super clamp (left) and then holding crack width using a small clamp (right).....	24
Figure 13. Crack in a mortar sample captured by camera (left) and crack retrieved by CAD software (right) .....	24
Figure 14. Top surface of mortar samples with different crack sizes .....	25
Figure 15. Top surface of mortar samples with different crack sizes captured by CAD software.....	26
Figure 16. Process of crack repair using the MICP method: Samples in UPB solution (upper left), samples in urea- $\text{CaCl}_2$ solution (upper right), and process sketch (bottom).....	28
Figure 17. Relationship between the crack width and crack area of mortar samples .....	30
Figure 18. Cracks in mortar samples after 7 cycles (left), 14 cycles (right), and 21 cycles (bottom) of MICP treatment .....	31
Figure 19. Effect of initial crack size on permeability of mortar samples after MICP treatment (left) and water treatment (right) .....	32
Figure 20. Relationship between permeability and cycles time during MICP treatment (top) and water treatment (bottom) .....	33
Figure 21. Splitting stress-strain curves of repaired samples with different crack sizes: average crack width < 0.25 mm (top left), average crack width = 0.25-0.52 mm (top right), average crack width = 0.62-1.09 mm (bottom left), and average crack width > 1.09 mm .....	34
Figure 22. Relationship between crack width and precipitated $\text{CaCO}_3$ content .....	35
Figure 23. Relationship between tensile strength and $\text{CaCO}_3$ content (top) and initial average crack width (bottom) .....	36

Figure 24. Precipitated  $\text{CaCO}_3$  on the cracked surface of mortar sample B14: crack surface of the split sample (top left), 12X magnification of the crack surface (top right), 50X magnification (middle left), 150X magnification (middle right), 500X magnification (bottom left), and 1,500X magnification (bottom right).....37

Figure 25. Coarse hexagon-shaped  $\text{CaCO}_3$  observed on the cracked surface of sample B15 at 500 times the actual size (left) and at 1,500 times the actual size (right) .....38

**LIST OF TABLES**

Table 1. Summary of engineering properties of MICP-treated sand in geotechnical applications .....5

Table 2. Summary of MICP applications in cement-based materials.....9

Table 3. Chemical characterization of SF5.....12

Table 4. Test results of solution A made with different limestone powder-to-SF5 ratios.....12

Table 5. Components in the final calcium solution (Solution D) .....13

Table 5. Test results of biocemented sand using the calcium solution made with limestone powder and SF5 .....16

Table 6. Crack sizes and test results of all cracked mortar samples studied .....29



## **ACKNOWLEDGMENTS**

The authors would like to thank the Midwest Transportation Center and the U.S. Department of Transportation Office of the Assistant Secretary for Research and Technology for sponsoring this research. The Iowa Department of Transportation (DOT) and Iowa Highway Research Board provided match funds for this project. The authors would like to acknowledge the Iowa DOT Office of Construction and Materials for their encouragement and in-kind support.

Special thanks are given to Jian Chu of Nanyang Technological University, Singapore for his valuable input on the entire project and Xuefei Zhao of the Department of Food Science at Iowa State University for her hands-on help in making soluble calcium solutions as well as her constructive advice on the development of microbiologically induced calcium carbonate precipitation using an acetic acid-rich solution. Undergraduate students Yu Tian, Civil Engineering, and Tiantian Ouyang, Food Science, also participated in the preparation and testing of biocemented sand made with the soluble calcium solution obtained from the limestone powder and acetic acid-rich solution.

The project would not have been successfully completed without the support and hard work of the above-mentioned groups and individuals.



## EXECUTIVE SUMMARY

Due to its environmental and economic benefits, biocementation resulting from a microbiologically induced calcium carbonate precipitation (MICP) process is being increasingly used to enhance civil infrastructure—through stone surface protection, sand cementation, soil consolidation, crack remediation, and so forth. In the MICP process, urease-producing bacteria (UPB) produce a urease enzyme that converts urea into ammonium ions and carbonate. In the presence of calcium ions, the calcium carbonate ( $\text{CaCO}_3$ ) precipitates, fills pores and cracks, forms salt bridges, and bonds loose particles together.

The present study was aimed at developing an eco-friendly, cost-effective biocement/grout for concrete/mortar crack repair using industrial and agricultural by-products. It included two main tasks: biocement/grout development and mortar crack repair.

For the biogROUT development, a urease-producing bacteria called *Bacillus sphaericus* (*sp.*) was selected to produce the urease enzyme. Instead of using the reagent grade calcium chloride ( $\text{CaCl}_2$ ), a calcium ion was produced by dissolving a limestone powder in an acetic acid-rich solution, which was derived from the pyrolysis of lignocellulosic biomass. This solution was called acetic acid-rich stage fraction 5, or SF5, in the present study. Efforts were made to optimize the calcium ion production through adjusting the limestone powder-to-SF5 ratio and the potential of hydrogen (pH) of the resulting solution.

In the study of crack repair, mortar cylinder samples were prepared and subjected to different levels of splitting tensile loads to generate different crack sizes in the samples. Different amounts of UPB and calcium solutions were then applied to the cracked mortar samples using different procedures to obtain the optimal MICP process. To investigate the effectiveness of the MICP repair process, the repaired mortar samples were tested for water permeability and splitting tensile strength (TS). The results were analyzed to find the relationship between the initial crack width and the amounts of calcium carbonate content in the mortar cracks. The following are the major findings from the present study:

1. The soluble calcium solution for MICP can be achieved from dissolving a limestone powder in an acetic acid-rich SF5 solution of biomass fast pyrolysis products. The properties of the soluble calcium solution for MICP was optimized based on the limestone powder-to-SF5 ratios, pH values of the obtained solutions, and procedures for applying the UPB and media (urea/calcium solutions) for  $\text{CaCO}_3$  precipitation (MICP treatment). The optimal 0.3 M calcium solution obtained from the present study consists of limestone, SF5, sodium hydroxide (NaOH), and distilled water, which equaled 1:8:0.045:13 by weight. Using such a soluble calcium solution made with industrial and waste by-products as a replacement for the  $\text{CaCl}_2$  in the MICP process provided desirable  $\text{CaCO}_3$  precipitation.
2. The properties of the sand samples cemented using the developed soluble calcium solution are comparable to those of the sand samples cemented using  $\text{CaCl}_2$  as a calcium source for MICP. The  $\text{CaCO}_3$  content of the sand samples biocemented using the new calcium source ranged from 5.67 to 8.19%. The permeability of the biocemented sand ranged from  $8.17\text{E-}6$

to  $1.52\text{E-}6$  m/s, unconfined compressive strength (UCS) ranged from 858 to 1,111 kPa, TS ranged 137 to 197 kPa, UCS/TS ratios ranged from 4.6 to 6.9, and the secant modulus of elasticity,  $E_{50}$ , was  $38.3\pm 1.7$  MPa for compression and  $24.3\pm 2.7$  MPa for tension.

3. Cracks in the mortar samples were repaired using the MICP technology, which gradually healed samples with each increasing treatment cycle. After being treated for 7 cycles, most small cracks ( $<0.52$  mm) were healed. After 21 cycles, all cracks (with an average width of 0.15 to 1.64 mm) were healed with a 1/16 to 1/8 in. of precipitated  $\text{CaCO}_3$  layering the top surfaces of repaired cylinders.
4. MICP repair technique can significantly reduce water permeability of cracked samples. Before any MICP treatment, the cracked mortar samples, with crack size ranging from 0.15 to 1.64 mm, had permeability values ranging from  $3.027\text{E-}3$  to  $9.237\text{E-}6$  m/s. After being treated with MICP for 7 cycles, their permeability decreased to the range of  $8.254\text{E-}5$  to  $2.046\text{E-}6$  m/s. After being treated with MICP for 21 cycles, the permeability of the mortar samples was only around  $1.000\text{E-}6$  m/s or less.
5. The splitting tensile strength of the MICP-repaired samples ranged from 32 to 386 kPa. However, the water treated mortar samples were all broken into two pieces after demolding and were therefore unable to be tested for TS. There was no clear relationship between TS and the  $\text{CaCO}_3$  content, as the samples had an average crack width of  $\leq 0.5$  mm. However, a clear relationship was observed for the sample average crack width of  $>0.52$  mm, where TS increased with  $\text{CaCO}_3$  content.
6. The scanning electron microscope (SEM) study suggested that there were two different forms of  $\text{CaCO}_3$  in the cracked mortar samples: flower-shaped clusters made with well-arranged thin (plate/sheet-like) hexagon  $\text{CaCO}_3$  (possibly vaterite) and granular clusters made with thick or coarse hexagon  $\text{CaCO}_3$  (probably calcite). The  $\text{CaCO}_3$  crystals had a size ranging from 5 to 20  $\mu\text{m}$ , which formed a porous matrix that filled in the cracks.

# 1 INTRODUCTION

## 1.1 Background

Cement-based materials have often been used for infrastructure construction and repair. The production of conventional Portland cement is energy-consuming and environmentally unfriendly. For example, production of one ton of Portland cement generates approximately one ton of carbon dioxide ( $\text{CO}_2$ ) from calcining limestone and fuel use. It is estimated that cement production contributes 7% of total global  $\text{CO}_2$  emissions. In recent years, an emerging material called biocement has been developed through a microbiologically induced calcium carbonate precipitation (MICP) process. Biocement is generally made of calcium salt, a small amount of urea, and urease-producing bacteria (UPB).

The most commonly used calcium salt for MICP is calcium chloride ( $\text{CaCl}_2$ ). Not only is  $\text{CaCl}_2$  expensive, but excessive  $\text{CaCl}_2$  in concrete can alter its properties and be harmful to human health and agriculture (Chung et al. 2014). Some studies have been performed to replace  $\text{CaCl}_2$  with different calcium sources, such as calcium hydroxide ( $\text{Ca}(\text{OH})_2$ ), calcium nitrate ( $\text{Ca}(\text{NO}_3)_2$ ), calcium acetate ( $\text{Ca}(\text{CH}_3\text{COO})_2$ ), and eggshell in vinegar (Choi et al. 2016a). The goal of this study was to develop an eco-friendly, cost-effective biogrout for concrete/mortar crack repair using industrial and agricultural by-products.

## 1.2 Objectives

The following specific objectives were designed to reach the above-mentioned project goal:

- Produce a soluble calcium source for MICP utilizing an industrial by-product, limestone fines, an agricultural by-product, and an acetic acid-rich fraction of biomass pyrolysis product
- Study the influences of bacterial quantity, available nutrients, and water content on the MICP process and maximize the biogenic calcium carbonate ( $\text{CaCO}_3$ ) productivity
- Evaluate the crack-healing effectiveness and ensure that concrete/mortar repaired with the newly developed biogrout has improved engineering properties

## 2 LITERATURE REVIEW

### 2.1 Microbiologically Induced Calcium Carbonate Precipitation

In the MICP process, UPB generally produces a urease enzyme that converts urea ( $\text{CO}(\text{NH}_2)_2$ ) into ammonium ( $\text{NH}_4^+$ ) as well as carbonate ions ( $\text{CO}_3^{2-}$ ). In the presence of calcium ions ( $\text{Ca}^{2+}$ ), the  $\text{CaCO}_3$  precipitates. In a biogROUT, UPB cells tend to attach to the surface of sand particles thus the genetic  $\text{CaCO}_3$  formed from MICP often covers sand particle surfaces, fills pores and cracks, creates salt bridges, and bonds loose particles together.

Equations 1-3 or 4 present the principles (i.e., chemical reactions) of the MICP process.



Or



Figure 1 illustrates the concept of biocementation resulting from the MICP process.

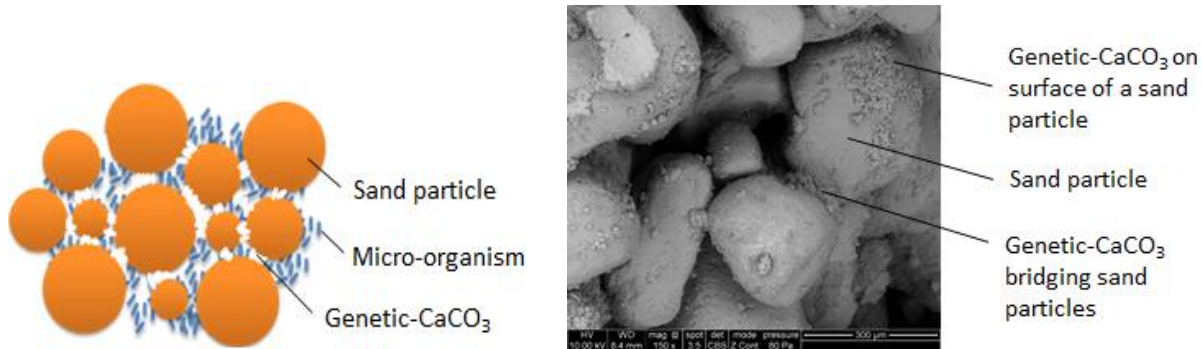


**Figure 1. Concept of biocementation (left) and sample of biocemented sand (right) from MICP**

The effectiveness of a MICP process is mainly governed by four elements: (1)  $\text{Ca}^{2+}$  concentration, (2) dissolved inorganic carbon (DIC) concentration, (3) potential of hydrogen (pH), and (4) availability of nucleation sites. These elements are in turn affected by the type and concentration of bacteria, nutrients, and reagent supplied in the system (Ng et al. 2012). In addition, processing procedures (e.g., mixing and injection) and environmental conditions (e.g.,

salinity and temperature) also have significant influences on MICP. The key in developing an effective  $\text{CaCO}_3$  precipitating biocement is to properly balance these factors.

## 2.2 Applications of MICP in Earth Materials

Biocementation using MICP has been increasingly applied in different areas of civil engineering since 2000. Mitchell and Santamarina (2005) reported that MICP could be easily applied to earth materials due to the size of the bacteria, which is typically 0.5 to 3.0  $\mu\text{m}$  and within the same range of pore sizes found in fine sand. As a result, bacteria have difficulties passing the pore throats of fine soils in nature and would be entrapped there during formation. Most biological activities would occur in silt, coarse sands, or rock fractures, where the unhindered microbial motion would occur and nutrients would be easy to transport.

Researchers have discovered that the MICP process improves strength, stiffness, and the impermeability of soils, and that improvements were directly related to the amount of  $\text{CaCO}_3$  formed during the MICP process (Whiffin et al. 2007). Van Paassen et al. (2010) tested large-scale biogROUT (100  $\text{m}^3$ ) and reported that the unconfined compressive strength (UCS) of the mortar was 0.7 to 12.4 MPa in comparison to the 12.6 to 27.3% of  $\text{CaCO}_3$  content. The elastic modulus ( $E_{50}$ ) of the sand also increased with the increasing  $\text{CaCO}_3$  content. Recently, Zhao et al. (2014) studied the effects of bacteria, urea, and  $\text{CaCl}_2$  concentration on the engineering properties of biocemented sand and found that UCS of the biocemented sand increased with urea reactivity as well as  $\text{CaCO}_3$  content.

Al Qabany and Soga (2013) investigated effects of urea and  $\text{CaCl}_2$  concentrations on the effectiveness of MICP. Their results showed that the use of a high concentration solution resulted in a rapid drop in permeability at the early stage of calcite precipitation. However, low concentration solutions provided the biocemented sand with higher strength due to the smaller size of  $\text{CaCO}_3$  formed during the MICP process, which also provided uniformed cementation.

Ivanov et al. (2010) developed biogROUT using ferric salts instead of the commonly used  $\text{CaCl}_2$  and investigated the effect of air curing and oven-dry curing on strength development. They found that the maximum UCS reached 800 kPa for an air-dried sample but became about 1500 kPa as the ferric hydroxide-to-sand ratio (by mass) reached 12%.

Li et al. (2015) demonstrated that the addition of homopolymer polypropylene multifilament fiber (0.1, 0.2, 0.3, 0.4, and 0.5% by weight of sand) to sand significantly improves the shear strength, ductility, and failure strain of the MICP-treated sand-fiber composite. The optimum fiber content was about 0.2 to 0.3%. Choi et al. (2016b) studied the effects of polyvinyl alcohol (PVA) fiber (at 0, 0.4, and 0.8% by weight of sand) on UCS, splitting tensile strength (TS), and permeability of biocemented sand. They found that fibers helped to refine the pores among sand particles and increase the amount of precipitated  $\text{CaCO}_3$  in the sand, thus significantly increasing strength and reducing permeability of the biocemented sand.

As mentioned previously, most studies use  $\text{CaCl}_2$  as a calcium source for MICP, which is expensive and environmentally unfriendly. Therefore, some studies were performed to replace  $\text{CaCl}_2$  with a different calcium source. Park et al. (2014) studied MICP using a plant extract (jack bean) to facilitate urease activity and  $\text{CaCl}_2$ , calcium hydroxide ( $\text{Ca}(\text{OH})_2$ ), and calcium nitrate ( $\text{Ca}(\text{NO}_3)_2$ ) for sand cementation. They found that the UCS of biocemented sand increased with increasing amounts of urea. The samples treated with a calcium solution made from  $\text{CaCl}_2$  had the highest  $\text{CaCO}_3$  content as well as the highest UCS when compared with samples treated with a calcium solution made from  $\text{Ca}(\text{OH})_2$  and  $\text{Ca}(\text{NO}_3)_2$ .

Zhang et al. (2014) studied MICP using  $\text{CaCl}_2$ ,  $\text{Ca}(\text{NO}_3)_2$ , and calcium acetate ( $\text{Ca}(\text{CH}_3\text{COO})_2$ ). They found the samples treated with a calcium solution made from  $\text{Ca}(\text{CH}_3\text{COO})_2$  had the highest UCS and recommended using  $\text{Ca}(\text{CH}_3\text{COO})_2$  as an alternative calcium source for the MICP technology when applied in the steel-reinforced materials.

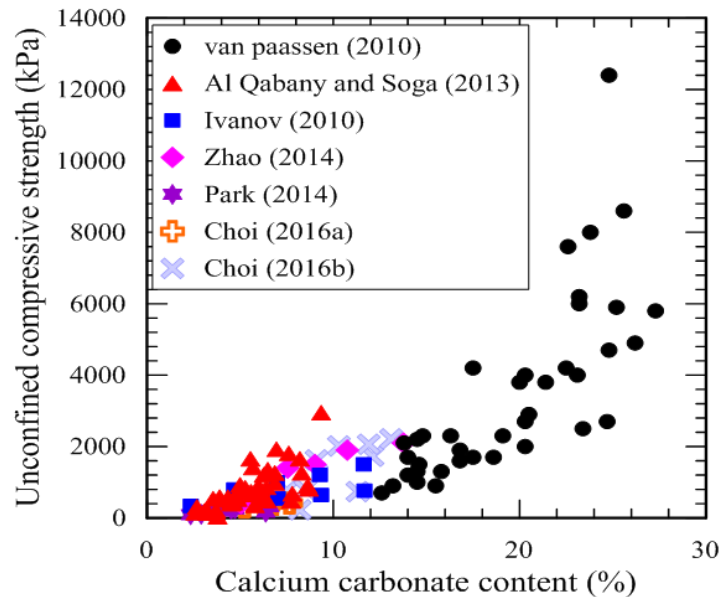
Choi et al. (2016a) used eggshell, a waste material, and vinegar as a calcium source for MICP. They found that for the same calcium ion concentration, the sand samples treated with the calcium solution made from eggshell and vinegar as a calcium source had higher UCS than samples treated with the calcium solution made from  $\text{CaCl}_2$ .

Table 1 summarizes the key parameters (i.e., materials and chemical concentrations) of the above-mentioned MICP studies as well as the major engineering properties of the MICP-treated earth materials.

**Table 1. Summary of engineering properties of MICP-treated sand in geotechnical applications**

No.	Bacteria	Chemical concentration (M)		CaCO <sub>3</sub> (%)	Strength (kPa)	Permeability (m/s)	References
		Urea	Calcium				
1	<i>Sporosarcina pasteurii</i>	1.1	1.1	17-105 (kg/m <sup>3</sup> )	190–574	2E-4–4E-5	Whiffin et al. 2007
2		1	0.05	12.6–27.3	700–12,400		Van Paassen et al. 2010
3		0.1–1.0	0.1 -1.0	2.6–9.3	0–2,950	<1.5E-4	Al Qabany and Soga 2013
4		0.25–1.5	0.25 -1.5	5.0–13.8	400–2,100		Zhao et al. 2014
5	Unknown				340–1,500		Ivanov et al. 2010
6	<i>Sporosarcina pasteurii</i>	0.2	0.2	6.6–8.0	70–175		Li et al. 2015
7	Plant extract (Jack bean)	1.7–8.0	1.8	2.34–6.58	90–317		Part et al. 2014
8	<i>Sporosarcina pasteurii</i>	0.5	0.5		11,200–43,000		Zhang et al. 2014
9		0.4	0.4	5.2–7.7	291–418	6.5E-6–1.0 E-6	Choi et al. 2016a
10		0.3	0.3	7.5–13.1	230–1,728	5.7E-5–9.9E-7	Choi et al. 2016b

Figure 2 summarizes the relationship between  $\text{CaCO}_3$  content and UCS based on the results reported in the above reviewed literature.



**Figure 2. Effect of  $\text{CaCO}_3$  content on the UCS of MICP-treated sand**

As seen in Figure 2, the UCS of biocemented sand increases linearly with  $\text{CaCO}_3$  content when  $\text{CaCO}_3$  content is lower than 15% and increases exponentially when  $\text{CaCO}_3$  content is higher than 15%. This suggests that genetic  $\text{CaCO}_3$  content plays a very important role in the engineering properties of biocemented materials.

### 2.3 Applications of MICP in Concrete Materials

Research has been conducted to improve the strength of concrete and mediate concrete cracks using MICP technology since genetic  $\text{CaCO}_3$  can fill the pores and spaces in concrete. The challenge is that some bacteria may not survive in high alkaline concrete mixtures. After exploration, researchers found that the bacteria *bacillus cohnii* and *bacillus sphaericus* (*sp.*) both possess high alkaline resistance and are suitable for being mixed in concrete mixtures (Dhami et al. 2013). In most cases, the bacteria are protected by storing them in spores or coating them with organic compounds like yeast extract, peptone, calcium acetate and calcium lactate. Through the MICP process, the produced genetic  $\text{CaCO}_3$  fills the pores in the concrete mixture so as to improve concrete strength. For concrete crack repair, bacteria *bacillus sp.* and *bacillus sphaericus* are often used due to its capacity for producing  $\text{CaCO}_3$  (Dhami et al. 2013).

De Muynck et al. (2008) used *bacillus sphaericus* (LMG 225 57) to improve concrete surface durability. Samples were treated with two types of solutions. First, concrete samples were soaked in the bacteria culture. After 1 day, they were taken from the culture and their surfaces were dried with a towel. Second, the samples were soaked in a solution made with different calcium sources ( $\text{CaCl}_2$  or  $\text{Ca}(\text{CH}_3\text{COO})_2$ ). The precipitated  $\text{CaCO}_3$  was found on the samples' surfaces

and resulted in a 65 to 90% reduction in water absorption, depending on the porosity of the specimens.  $\text{CaCl}_2$  for biocement measured higher TS than  $\text{Ca}(\text{CH}_3\text{COO})_2$  as a calcium source.

Jonkers et al. (2010) developed self-healing concrete using *bacillus pseudofirmus* (DSM 8715) and *bacillus cohnii* (DSM 6307). In their study, Portland cement was mixed with water and washed cell ( $1-10 \times 10^8/\text{cm}^3$ ). They found that the hardened samples made with bacteria had lower compressive strength than the control samples (without the addition of bacteria). The addition of various organic compounds (such as yeast extract, peptone, and calcium acetate) decreased strength further, but the addition of calcium lactate increased the paste strength at 28 days, which contributed to an increase in precipitated  $\text{CaCO}_3$  content.

Vempada et al. (2011) developed a MICP-modified mortar using various microbiological isolates (*bacillus substilis JC3* and *salinicoccus sp.* and *E. coli*). They introduced bacteria at different cell concentrations into cement mortar specimens and compared the strength of the mortar samples. They found that except for *E. coli*, all the other bacteria isolates enhanced the mortar strength. Out of all isolated cultures, *bacillus substilis JC3* offered the best improvement in compressive strength.

Pei et al. (2013) incorporated *bacillus subtilis* into a concrete mixture and studied the three different amounts of live and dead cells ( $3.3 \times 10^{-3}$ ,  $3.3 \times 10^{-1}$ , and  $3.3 \times 10^1$ ) in the concrete system. They considered both time and the effect of different liquid media ( $\text{CaCl}_2$ , sodium bicarbonate, ammonium chloride, both nutrients, and urea). They found that by mixing live cells in mortar helped to develop strength. But, the use of dead cells in mortar actually decreased strength. The type of liquid media had no statistically significant effect on the concrete strength at both 7 and 28 days.

Ramachandran et al. (2001) incorporated *bacillus pasteurii* and *pseudomonas aeruginosa* into a freshly mixed cement paste with different concentrations of live and dead cells (0,  $3.0 \times 10^7$ ,  $6.0 \times 10^7$  and  $1.2 \times 10^8/\text{cm}^3$ ). After 24 hours, the hardened samples were placed in 3 liters of urea- $\text{CaCl}_2$  with 2 grams of lime. This study showed that the compressive strength of the hardened cement paste with incorporated live bacteria increased by 10 to 30% at 7 days. Mixing these two live bacteria provided a synergistic effect and the highest UCS. The dead bacteria in the paste system did not help the paste strength improvement.

Van Tittelboom et al. (2010) studied concrete crack repair using biogROUT made with different materials: *bacillus sphaericus* in sol-gel with  $\text{Ca}(\text{NO}_3)_2$  or  $\text{Ca}(\text{CH}_3\text{COO})_2$  and autoclaved *bacillus sphaericus* in sol-gel with  $\text{Ca}(\text{NO}_3)_2$  or  $\text{Ca}(\text{CH}_3\text{COO})_2$ . Cracks of 0.1 to 0.9 mm in width were generated in the concrete samples (150 mm x 150 mm x 70/150/600 mm) by pre-inserting a copper plate in the samples and through mechanical loading. The cracks in the samples were repaired by first applying the biogROUT as a sealing material on the cracks and then soaking the samples in the sol-gel with different chemicals:  $\text{CaCl}_2$ ,  $\text{Ca}(\text{NO}_3)_2$ , and  $\text{Ca}(\text{CH}_3\text{COO})_2$ . They observed that all cracks filled when bacteria were protected by the silica gel. The permeability of the samples subjected to biogROUT treatment significantly decreased when compared with that of samples without treatment. However, the treatment without *bacillus sphaericus* in sol-gel was not able to mediate the cracks.

Abo-El-Enein et al. (2012) repaired mortar cracks by injecting biocement made with *bacillus sp.*, urea, and various chemicals ( $\text{CaCl}_2$ ,  $\text{Ca}(\text{CH}_3\text{COO})_2$  and  $\text{Ca}(\text{NO}_3)_2$ ). Three types samples were prepared and tested for compressive strength at 28 days: (1) control (uncracked sample), (2) untreated (cracked sample), and (3) treated by bacterial cell (repaired sample). They found that compressive strength of the untreated mortar was lower than that of the control sample by 43%, while the bacteria treated samples possessed strengths only 10% lower than that of the control sample.

Later, Achal et al. (2013) studied the effects of crack depth and *bacillus sp.* concentration on crack repair. Three different cracks (13.4, 18.8, and 27.2 mm) and three different bacteria concentrations ( $5 \times 10^{-6}$ ,  $5 \times 10^{-7}$ , and  $5 \times 10^{-8}$ ) were used for MICP by the chemicals urea and  $\text{CaCl}_2$ . They found that all samples treated with bacteria had higher UCS than untreated specimens. The UCS of bacteria-treated samples decreased slightly with increasing crack width. The samples treated with  $5 \times 10^{-7}$  bacteria concentration had the highest UCS, followed by the samples treated with  $5 \times 10^{-8}$  bacteria concentration and then the samples treated with the  $5 \times 10^{-6}$  bacteria concentration.

Wang et al. (2014) studied repair of mortar with different crack areas (0 to  $160 \text{ mm}^2$ ) using *bacillus sp.* and various chemicals (yeast extract, urea, and  $\text{Ca}(\text{NO}_3)_2$ ). The mortar samples were made with cement and water containing 0, 1, 2, 3, 4 and 5% centrifuged bacteria. At 28 days, a uniaxial tensile load was applied to the specimens at a strain rate of 0.01 mm/s until the average crack width of the specimen reached 150  $\mu\text{m}$ . The mortar samples were then immersed in different solutions: water, deposition medium, wet-dry cycles in water, and wet-dry cycles with urea and  $\text{Ca}(\text{NO}_3)_2$ . They found that the permeability of the samples soaked in the urea and  $\text{Ca}(\text{NO}_3)_2$  solution decreased almost 10 times faster than samples repaired with other solutions. However, the tensile strength and unconfined compressive strength of the samples did not increase.

Table 2 summarizes MICP applications in cement-based materials.

It should be pointed out that although some work has been done, study of concrete repair using MICP technology is still very limited. The above-mentioned studies have indicated that MICP can contribute to crack repair via several mechanisms: (1) filling cracks with biogenic  $\text{CaCO}_3$ , microbial biomass, and polysaccharides (formed through enzyme-catalyzed condensation); (2) bonding loose materials with biogenic  $\text{CaCO}_3$ , microbial biomass, and polysaccharides; and (3) forming salt bridges between particles and/or colloids mediated by microorganisms. It is expected that after being repaired with biocement/grout, cracked concrete can resume its integrity and have proper mechanical properties and water penetration resistance. Although the concept of MICP is promising, the repair materials and procedure used vary widely in different studies. The effect of crack width on MICP repair effectiveness is still not clear. More study is needed in order to improve and to apply MICP technology to field concrete repair applications.

**Table 2. Summary of MICP applications in cement-based materials**

<b>Application</b>	<b>Bacteria and Chemical Solutions</b>	<b>Cementation Method</b>	<b>Property Improvement</b>	<b>References</b>
Strength and property improvement for cement mortar	Bacteria and nutritional medium	Spray	Decreased permeability	Le Metayer-Levrel et al. 1999
	<i>bacillus pasteurii</i> and urea-CaCl <sub>2</sub> solution	-	-	Stocks-Fischer et al. 1999
		Mixing from concentrated cells	Increase strength up to 20 %	Ramachandran et al. 2001
	<i>bacillus subtilis</i> Urea solution	Circulation	Increase UC/TS strength	Choi et al. 2016b
		Mixing from concentrated cells	Increase UC strength up to 19 %	Vempada et al. 2011
			Increase UC strength up to 19%	Pei et al. 2013
<i>shewanella</i> and sterile solution	Mixing from concentrated cells	Increase UC strength 25%	Ghosh et al. 2005	
Remediation of cracks in concrete	<i>bacillus sphaericus</i> and growth/ biocementation medium	Immersion	Decrease of permeability	De Belie and De Muynck 2008
	<i>bacillus pasteurii</i> and urea-CaCl <sub>2</sub> solution	Immersion	Increase stiffness about 10%	Ramachandran et al. 2001
	<i>sporosarcina pasteurii</i> and urea-CaCl <sub>2</sub> solution	Injection	Increase UC strength 50%	Abo-El-Enein et al. 2012
Self-healing	<i>bacillus pseudifirmus</i> , <i>bacillus cophnii</i> , and calcium lactate solution	Mixing from concentrated cells and then cured	Increased UC strength with calcium lactate	Jonkers et al. 2010

### 3 RESEARCH APPROACH AND SCOPE

This study includes two main tasks: biogROUT development and mortar crack repair. For the biogROUT development, a urease-producing bacteria called *bacillus sp.* was selected to produce the urease enzyme. Calcium ions were produced in a solution using limestone fines and acetic acid-rich stage fraction 5, or SF5, instead of the conventionally used  $\text{CaCl}_2$  for the MICP process.

To study crack repair, mortar cylinder samples were prepared and subjected to different levels of splitting loads, thus generating different sizes of cracks (i.e., different crack areas and widths) in the samples. The repair technique was optimized by applying in different orders the amount of UPB and calcium solutions to the cracked mortar samples under varying environmental conditions. To investigate the effectiveness of the biogROUT repair or crack healing, the repaired mortar samples were tested for water permeability and splitting tensile strength.

## 4 BIOGROUT DEVELOPMENT

The biogrout development included four steps: (1) prepare materials and solutions for MICP tests, (2) perform MICP tests and confirm  $\text{CaCO}_3$  formation, (3) conduct MICP tests for sand cementation, and (4) evaluate engineering properties of the biocemented sand.

### 4.1 Preparing Materials and Solutions

The biogrout was made of UPB, urea, and a calcium solution produced via the MICP process. The UPB selected for the present study was *bacillus sp.* (ATCC 11859) (DeJong et al. 2006, Li et al. 2015, and Whiffin et al. 2007). The urea was purchased from Fisher Chemical. As mentioned previously, the calcium solution was made from dissolving a limestone powder in the acetic acid-rich SF5. The processes involved in the culturing of the UPB and making the calcium solution are described below.

#### 4.1.1 Bacteria Culture

To culture *bacillus sp.*, a medium was first prepared, which was made of a yeast extract (20 g), ammonium sulfate  $(\text{NH}_4)_2\text{SO}_4$  (10 g), and a 0.13 M Tris buffer (pH=9.0) solution. The *bacillus sp.* was sterilized in an autoclave at a temperature of 121°C for 15 minutes. Then, a small amount (3 to 5 ml/liters) of the sterilized microorganism was injected into the medium and cultured in a 30°C incubator for 2 days. After 2 days, the activity of the bacteria was tested to confirm its conditions.

To evaluate the activity of the bacteria, the optical density (OD) of the UPB solution was measured by a spectrophotometer. The measurement ranged from 1.0 to 1.6 (OD600), which is similar to results found by other researchers (Al Qabany and Soga 2013, Zhao et al. 2014). Second, urease activity of the UPB solution was measured using an electric conductometer (Stabnikov et al. 2013). The measurements ranged from 8 to 15 mM/min and was similar to or a little bit higher than other results (Zhao et al. 2014, Harkes et al. 2010).

#### 4.1.2 Preparation of Soluble Calcium Solution

The acetic acid-rich SF5 was received from the Bioeconomy Institute at Iowa State University in Ames, Iowa. Its chemical properties are presented in Table 3.

**Table 3. Chemical characterization of SF5**

Chemical Compounds	Weight (%)
Water	63.12
Acetic acid CH <sub>3</sub> COOH	7.53
Formic acid	1.22
Methanol	1.49
Furfural	0.20
Acetol	5.06
5-Hydroxymethylfurfural (HMF)	0.28
Total phenolics	2.09
Unknown compounds	19.01
Total	100.00

Zhao et al. 2013

The limestone powder used was a by-product from the Martin Marietta limestone quarry in Ames, Iowa. It had a particle size passing through the #200 sieve and a specific gravity of 2.70. The chemical properties of the limestone powder are listed in Table 4.

**Table 4. Test results of solution A made with different limestone powder-to-SF5 ratios**

ID	Limestone powder (g)	SF5 (ml)	Calcium concentration (Mol)	pH
LS10	10	20	0.83	5.2
LS40	10	40	0.80	5.1
LS80	10	80	0.76	5.0
LS120	10	120	0.64	4.8

Because the SF5 contained more than 7% acetic acid, it was expected to dissolve the limestone powder and produce a soluble calcium solution according to the following equation:



To make the soluble calcium solution, an optimal limestone-to-SF5 ratio was studied according to the following procedure:

1. First, 100 g of limestone powder was mixed with 400, 800, and 1200 ml of SF5 solution to form solutions with limestone powder-to-SF5 ratios of 1:4, 1:8, and 1:12 (designated as Solution A). After 5 days stored in a room temperature environment, calcium concentration and pH values of Solution A were measured. Table 4 shows the test results. The solutions where calcium concentration reached 0.7 to 0.8 M and the pH ranged between 0.4 and 0.45 were selected as candidates for further study.
2. Next, 1,300 ml of distilled water was added to each solution to ensure that their calcium concentrations reached 0.3 M (designated as Solution B).

3. Then, 4.5 g sodium hydroxide (NaOH) was added to Solution B to adjust the pH of each solution to a range of 7.0 to 7.5 (designated as Solution C).
4. Finally, Solution C was centrifuged using a speed of 4000 revolutions per minute (RPM) for 20 minutes to obtain a clear solution (designated as Solution D), which was considered the final optimal soluble calcium solution for biocementation. Table 5 summarizes the properties of Solution D (produced from the limestone powder and SF5).

**Table 5. Components in the final calcium solution (Solution D)**

<b>Limestone powder (g)</b>	<b>SF5 (ml)</b>	<b>NaOH (g)</b>	<b>Distilled water (ml)</b>	<b>Centrifuge</b>
100	800	4.5	1,300	4000 RPM, 20 min

#### 4.1.3 Determination of Calcium/Urea Ratio

Al Qabany and Soga (2013) discovered that the lower calcium concentration provided stronger biocementation. In this study, the calcium: urea=1:1 ratio was used and the calcium-urea concentration of 0.3 M was selected based on a previous study (Choi et al. 2016b)

## 4.2 MICP Tests and Precipitated CaCO<sub>3</sub>

The following procedure was used for the MICP tests in the present study:

1. Grow the UPB for 2 days to reach a density of 0.8 to 1.2 at OD600 nm.
2. Mix 0.3 M urea with the UPB solution at a ratio of urea:UPB=1:1.5 (by volume) in a test tube for 1 day (pH=8.5).
3. Add calcium solution to the UPB-urea solution (precipitation occurred immediately).

To evaluate the properties of the precipitated material, the precipitated material was filtered out and placed in a small container and oven dried at 115°C for 1 day. The dried precipitated material was then analyzed using x-ray diffraction (XRD). Figure 3 shows the precipitated material and Figure 4 shows the XRD result.

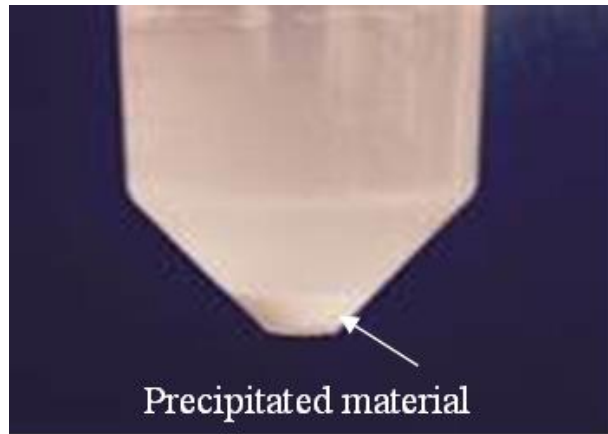


**Figure 3. Precipitated materials observed during MICP tests**

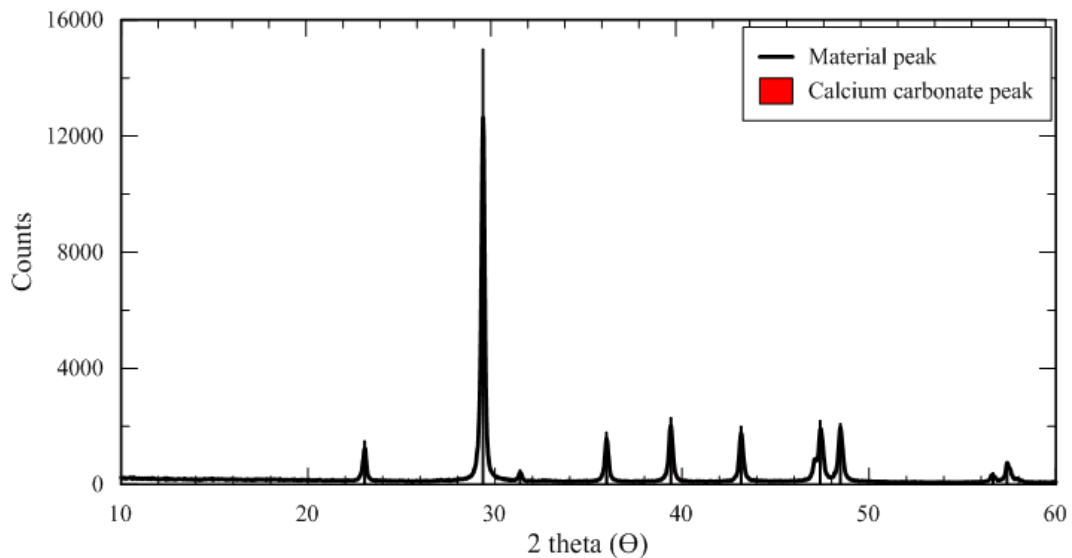


**Figure 4. XRD result of the precipitated material observed from the MICP using the calcium solution made from limestone powder and SF5**

It can be seen from Figure 4 that the XRD pattern of the precipitated material collected (black line) is overlapping with the XRD pattern of standard  $\text{CaCO}_3$  (red line). This confirmed that the precipitated material is  $\text{CaCO}_3$ .

### 4.3 MICP Test for Sand Cementation

#### 4.3.1 Preparation of Sand Samples

To prepare the biocemented sand samples, sand received from U.S. Silica Company's Ottawa plant in Ottawa, Illinois, was placed in a 5 cm by 10 cm plastic cylinder in 10 layers, and each layer was compacted until reaching a height of 1 cm. After compaction, the total height of each sand sample reached approximately 10 cm, and the unit weight of the sample reached

approximately  $1.70 \text{ g/cm}^3$ . Twelve samples were prepared, with six used to test UCS and six used to test TS.

#### 4.3.2 Application of MICP

To induce biocementation, a piece of 3M Scotch-Brite scouring pad was placed on each end of the sand samples as a filter. The samples, together with their plastic cylinder molds, were set on a funnel filled with gravel and held vertically with a sample holder. A cup was placed at the bottom of the sample to collect the solution as it penetrated through the sample (see Figure 5).

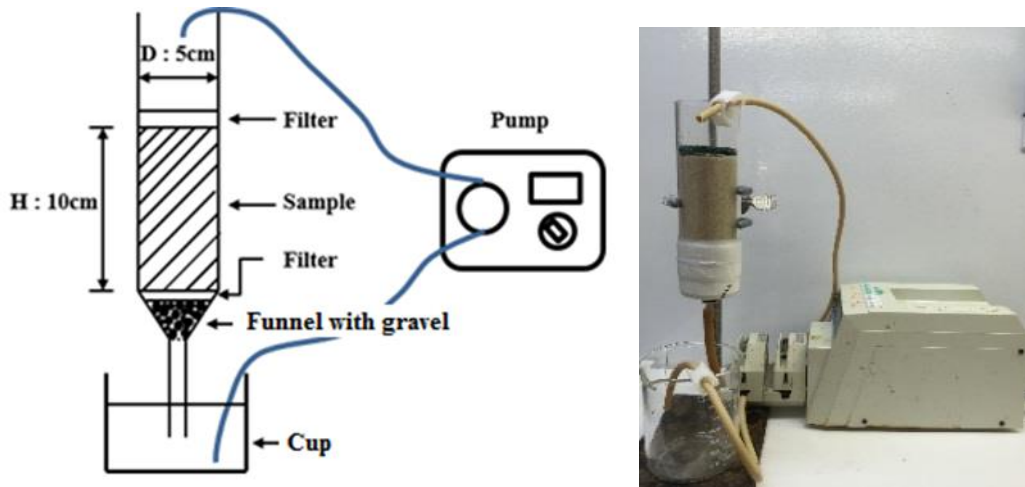


**Figure 5. Sketch of MICP test setup (left) and actual (right)**

The following procedure was used to apply UPB and urea/calcium solutions to the sand samples:

1. The first step included incubating 80 ml of the UPB solution for 2 hours and then pumping it onto the sand samples. The cup at the bottom collected the solution as it penetrated through the sample, so that the solution would be fully circulated.
2. After 3 hours of circulation, the UPB solution was discarded and replaced with the UPB-urea/calcium solution (UPB (30 ml)/urea (225 ml)/calcium (150 ml)) and circulated for 9 hours. Steps 1 and 2 form the first cycle of the UPB-urea/calcium circulation.
3. After the first cycle, freshly made UPB and UPB-urea/calcium solutions were circulated again.
4. Similar UPB-urea/ $\text{CaCl}_2$  solution circulations were repeated twice a day for 7 days. At this time, precipitated  $\text{CaCO}_3$  was generally observed in the tested samples (Choi et al. 2016b).

After 10 days of MICP treatment, the samples were washed with distilled water, the plastic cylinder molds were removed from the samples, and the samples were washed with water again. Figure 6 shows the cemented sample after washing.



**Figure 6. Cemented sand after MICP treatment**

#### 4.4 Evaluation of Properties of the Biocemented Sand

The properties of the evaluated biocemented sand samples included the amount of  $\text{CaCO}_3$ , water permeability, UCS, and TS. After finishing treatment, samples were soaked in distilled water for 1 day, and the water permeability of the samples was then determined by a constant head permeability test performed according to ASTM D 2434-68. After the permeability test, samples were put on a table in a concrete lab ( $23^\circ\text{C}$  and 50% RH) for one day to dry the samples. The UCS test was then determined according to ASTM D 4219 and the TS test conducted according to ASTM C 496. Small pieces of the broken samples were collected from the center for examination of their microstructures under a scanning electron microscope (SEM). In addition, the amount of  $\text{CaCO}_3$  in the biocemented sand samples was assessed according to ASTM D 4373. Table 5 includes the summarized test results.

**Table 5. Test results of biocemented sand using the calcium solution made with limestone powder and SF5**

ID	Type	CaCO3 content (%)	Permeability (m/s)	Strength (kPa)	Elastic Modulus ( $E_{50}$ , MPa)
UC1	UCS	6.39	3.18E-06	858	36
UC2		7.24	2.11E-06	1,062	39
UC3		7.54	1.52E-06	1,111	40
TS1	TS	5.67	8.17E-06	137	21
TS2		6.89	4.11E-06	148	25
TS3		8.19	1.73E-06	197	27
Average		6.99	3.47E-06	UCS:1,010 TS:161	UCS:38.3 TS:24.3

#### 4.4.1 Permeability and CaCO<sub>3</sub> Content

Permeability tests were performed on six sand cylinder samples before and after MICP tests. Before the MICP treatment, the permeability of the uncemented sand was approximately 1E-4 m/s. After the 10-day MICP treatment, the water permeability values of the biocemented sand ranged from 8.17E-6 to 1.52E-6 m/s, depending upon the CaCO<sub>3</sub> content of the samples. The CaCO<sub>3</sub> content of the samples ranged from 5.67 to 8.19%. As shown in Figure 7, permeability decreased with the CaCO<sub>3</sub> content of the samples, which is consistent with findings by other researchers (Chu et al. 2013 and Choi et al. 2016b).

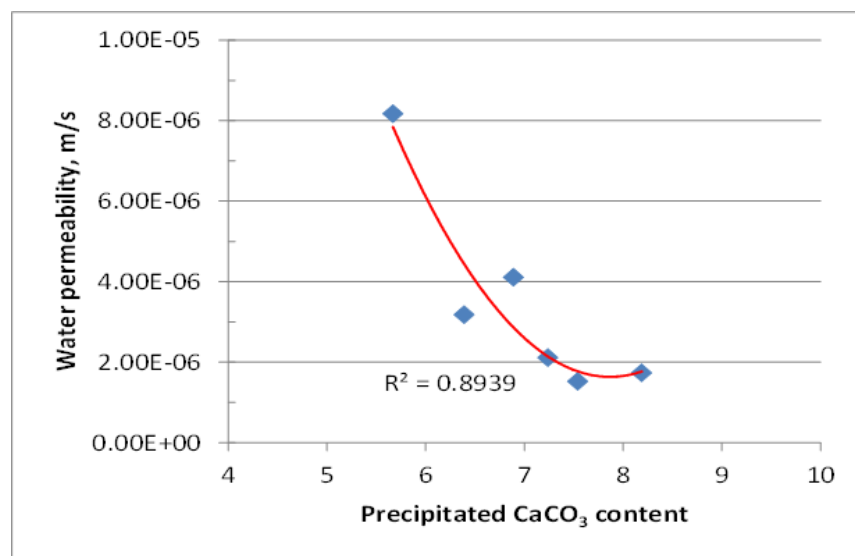


**Figure 7. Effect of CaCO<sub>3</sub> content on permeability of biocemented sand**

#### 4.4.2 Strength and Elastic Modulus

After permeability tests, the samples were placed on a table under a lab condition (approximately 23°C and 50% RH) to dry naturally for 2 days. Three of the six samples were then tested for UCS, and the other three samples were tested for TS. Figure 8 shows the stress-strain curves of the samples from the UCS and TS tests. Based on the test result,  $E_{50}$  was calculated from the stress-to-strain at the point where stress reached 50% of the UCS or TS.

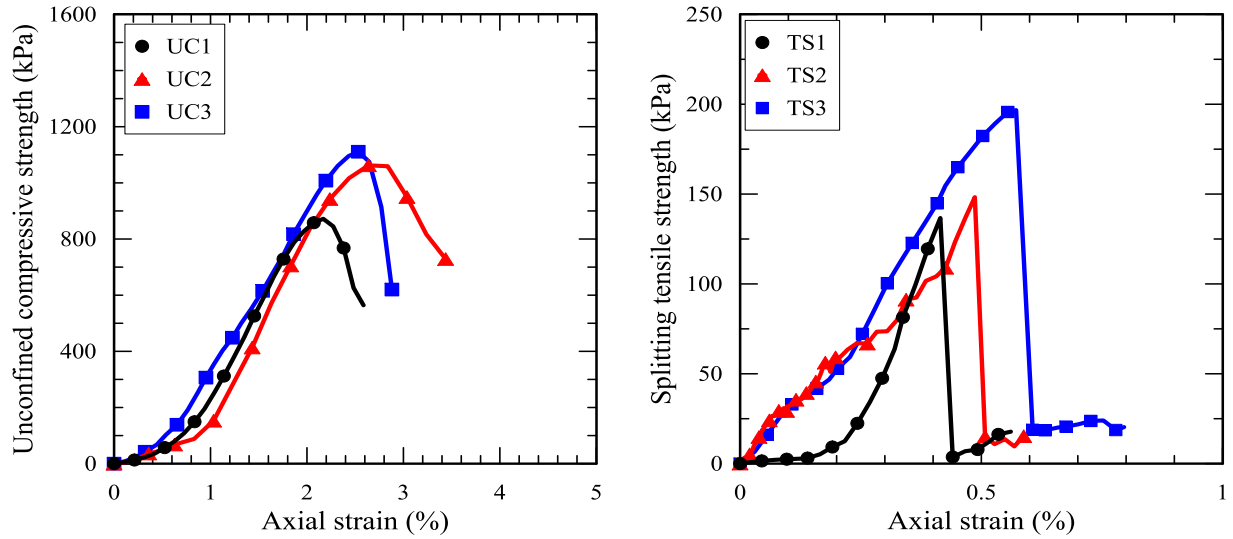


**Figure 8. Strain-stress relationships of biocemented sand showing UCS (left) and TS (right)**

The graph on the left in Figure 8 shows that, although treated under the same condition, the samples had different UCS. However, their stress-strain behavior is similar. As indicated earlier in Table 5, the elastic modulus of the three samples under compression was very close:  $E_{50}=38.3\pm 1.7$  MPa.

The graph on the right in Figure 8 shows that, under splitting tensile loading, three biocemented samples had different strength and stress-strain behavior. As indicated earlier in Table 5, the variation in the elastic modulus of the three samples under tension was relatively larger ( $E_{50}=24.3\pm 2.7$  Mpa). The measured UCS and TS ranged from 858 to 1,111 kPa and from 137 to 197 kPa, respectively. These strength values are comparable with those obtained from the biocementation using  $\text{CaCl}_2$  as a source of soluble calcium solution. For example, Al Qabany and Soga (2013) reported a UCS range of 500 to 1300 kPa obtained from biocemented sand with 4.0 to 6.5% of  $\text{CaCO}_3$  content made with 0.25 M of urea and  $\text{CaCl}_2$  solution.

Figure 9 illustrates the relationships between mechanical properties (UCS, TS, and  $E_{50}$ ) and the  $\text{CaCO}_3$  content of the samples tested in the present study.

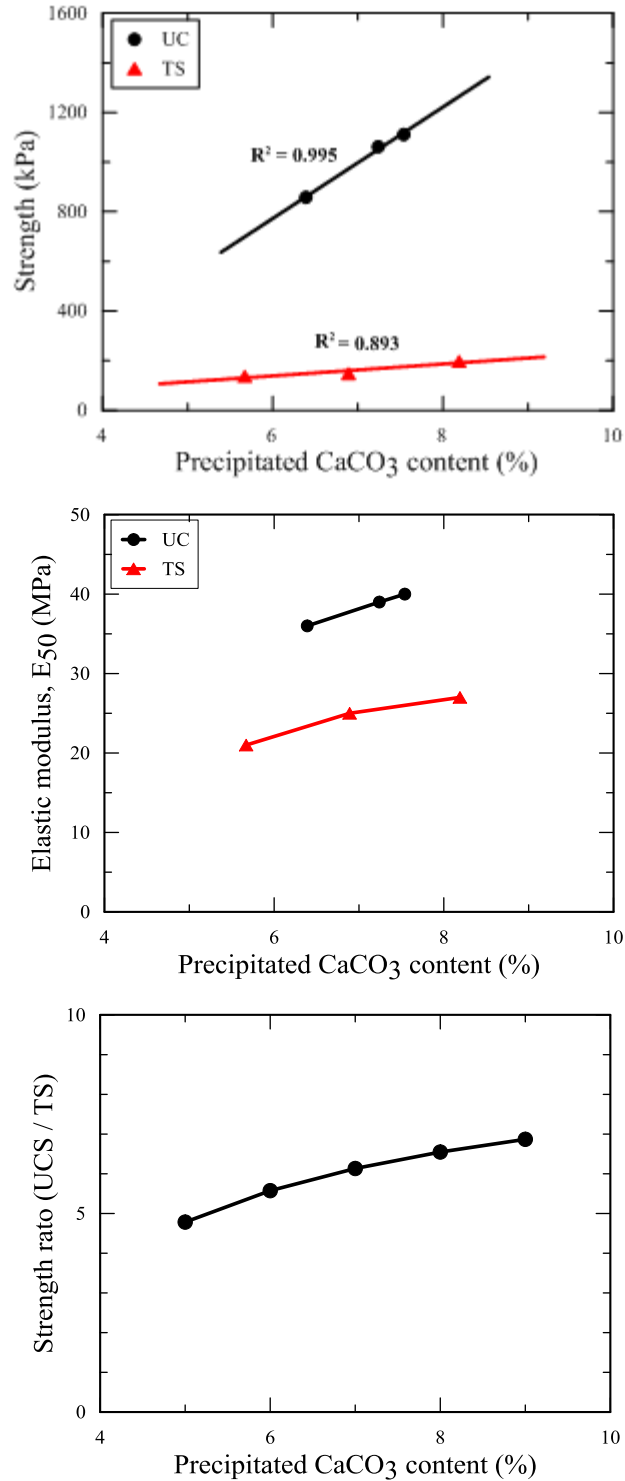


**Figure 9. Physio-mechanical properties of biocemented sand showing UCS (top), TS (middle), and UCS/TS ratio (bottom)**

The top graph in Figure 9 shows that both UCS and TS increased linearly with CaCO<sub>3</sub> content, which is also consistent with previous studies (Park et al. 2014, Whiffin et al. 2007, and Al

Qabany and Soga 2013). The middle graph in Figure 9 shows that  $E_{50}$  of the samples related well to the  $\text{CaCO}_3$  content. The elastic modulus increased with increasing  $\text{CaCO}_3$  content. And the bottom graph in Figure 9 demonstrates that the UCS/TS ratio of the samples ranged from 4.6 to 6.9, and the ratios also related well to the  $\text{CaCO}_3$  content.

According to Griffith (1924), the compression-to-tensile strength ratio describes the brittleness of a material, and the higher the ratio, the more brittle the material is. This strength ratio is about 8.0 for rock materials as well as for Portland cement-based materials. This suggests that the biocemented sand obtained from the present study is less brittle than the mortar made with conventional Portland cement.

#### 4.4.3 Microstructure

After UCS tests, small pieces of biocemented sand were examined under a SEM. Figure 10 shows the images from the SEM study.

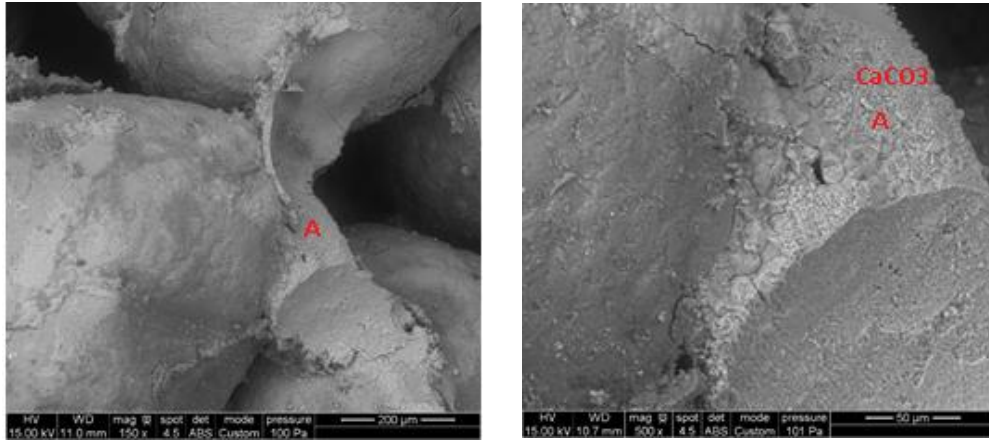


**Figure 10. Biocemented sand with two sand particles connected by  $\text{CaCO}_3$  (left) and cubic shaped  $\text{CaCO}_3$  (right) under a SEM**

The figure shows that, after the biotreatment, most of the sand particle surfaces were covered with  $\text{CaCO}_3$ , which provided a strong bond to cement the sand particle together. In addition, clusters of  $\text{CaCO}_3$  were observed, which filled the spaces between the sand particles and bridged the particles together. Such microstructure images of the biocemented sand samples further confirm the mechanisms of biocementation (Al Qabany et al. 2013 and Zhao et al. 2014).

#### 4.5 Summary

The results from the present study indicated that the soluble calcium solution used in the MICP process can be replaced by a new soluble calcium solution obtained from dissolving a limestone powder (i.e., a by-product from a limestone quarry) into an acetic acid-rich SF5 solution made from a waste material from a pyrolysis and bio-oil fractionation system. The properties of the soluble calcium solution for MICP can be optimized from the study of different limestone

powder-to-SF5 ratios, pH values of the obtained solutions, and procedures for applying the UPB and media (urea/calcium solutions) for  $\text{CaCO}_3$  precipitation (MICP treatment). Using such a soluble calcium solution to replace  $\text{CaCl}_2$  in the MICP process has provided desirable  $\text{CaCO}_3$  precipitation. The properties of the sand samples biocemented using the limestone-SF5 calcium solution are comparable to those of the sand samples reported in previous studies—where  $\text{CaCl}_2$  was used for MICP.

## 5 MORTAR CRACK REPAIR

### 5.1 Materials and Sample Preparation

#### 5.1.1 UPB Solution

The UPB selected for the present study was *bacillus sp.* (ATCC 11859), which is known to have strong urease activity (Chu et al. 2012 and Dejong et al. 2006). The medium for culturing *bacillus sp.* was made of a yeast extract (20 g), ammonium sulfate  $(\text{NH}_4)_2\text{SO}_4$  (10 g), and a 0.13 M Tris buffer (pH=9.0) solution (Zhang et al. 2014). After the medium was sterilized in an autoclave at 121°C for 15 minutes, the microorganism was injected into it and cultured in a 30°C incubator for 2 days. The activities of the bacteria were then tested.

To test the activities of the *bacillus sp.*, optical density of the culture was first measured by a spectrophotometer to estimate the growth and metabolic activity of the cells. The measurements ranged from 1.0 to 1.6 (by the standard OD600 nm in the spectrophotometer), which is similar to what was obtained by other researchers (Al Qabany and Soga 2013 and Zhao et al. 2014). Then, urease activity of the UPB was measured using an electric conductometer (Stabnikov et al. 2013). The measurements ranged from 8 to 15 mM/min, which is slightly higher than what was obtained by others (Zhao et al. 2014 and Harkes et al. 2010).

#### 5.1.2 Urea- $\text{CaCl}_2$ Solution

A 0.2 M urea- $\text{CaCl}_2$  solution was used for the MICP process, which was made according to the following procedure:

1. Dissolve 24.24 g of urea (solid) into 1.8 liters of water and then add more water to get a 2 liter/0.2 M urea solution.
2. Dissolve 44.39 g of  $\text{CaCl}_2$  (solid) into 1.8 liters of water and then add more water to get a 2 liter/0.2 M  $\text{CaCl}_2$  solution.
3. Mix the above 2 liter/0.2 M urea solution with the 2 liter/0.2 M  $\text{CaCl}_2$  solution to get a 4 liter/0.2 M urea- $\text{CaCl}_2$  solution.

#### 5.1.3 Mortar

Mortar samples were made of ordinary Portland cement (OPC), river sand, and distilled water. The water-to-cement ratio (w/c) of the mortar was 0.4 and the sand-to-cement ratio (s/c) was 2.5. The OPC had a specific gravity of 3.15 and Blaine fineness of 330 m<sup>2</sup>/kg. The sand had a specific gravity of 2.64 and a fineness modulus of 2.69. The TS of the intact mortar was 2,242 kPa after 7 days of standard curing (23°C and >95% RH).

To mix the mortar, the cement was first added into water and mixed by hand for 1 min. Sand was then added into the mixture and mixed for another 2 mins. The freshly mixed mortar was poured into 5 cm (in diameter) by 10 cm (in height) plastic cylinder molds in 2 layers, with each layer rodded 25 times. After casting, the cylinders were placed in a lab environment (under a temperature between 20 and 24°C) for 21 days before being cracked.

#### 5.1.4 Cracked Mortar Samples

In order to make a single straight crack in the mortar sample, two half rods (12.5 mm in diameter and 10.16 cm in length), attached with a thin metal wire (0.75 mm in diameter) on the tips, were glued to the end of the cylinder mold (see Figure 11).

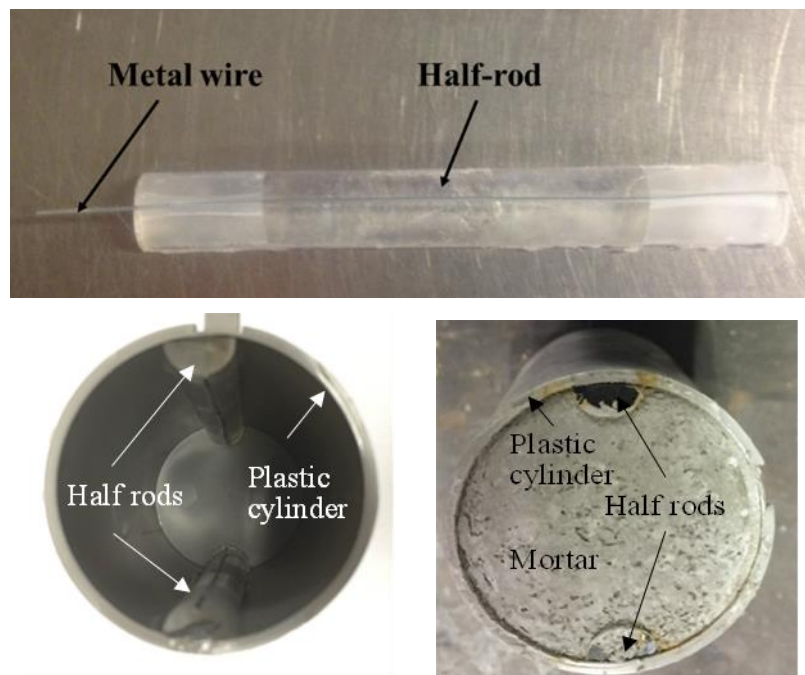


**Figure 11. Preparation of cylinder mold for mortar sample casting: metal wires attached on half rods (top), half rods in cylinder mold (left), and half rods in cast mortar sample (right)**

After mortar samples were cast and cured for 21 days, 25 cm discs were cut from each end of a mortar sample, and the middle section of the sample was cut again to make two short cylinder samples (5 cm in diameter and 4 cm in height). Each of these small cylinder mortar samples (5 cm x 4 cm), with its plastic mold on, was placed in a super clamp as shown in Figure 12. Through clamping, a force was applied to split the sample slowly and make a designed crack width. The cracked mortar sample was then transferred into a small clamp so as to keep the crack open (see image on the right in Figure 12).

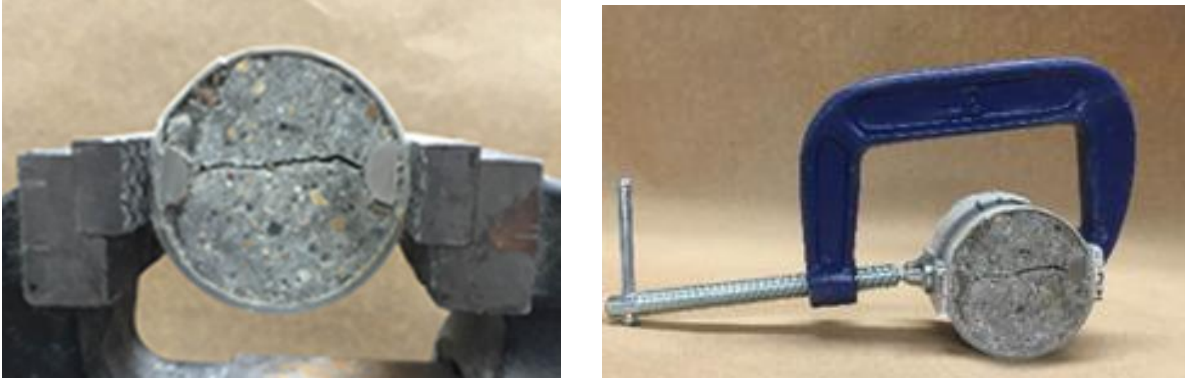


**Figure 12. Making a crack in a mortar sample by splitting mortar using a super clamp (left) and then holding crack width using a small clamp (right)**

After 7 days, the small clamps were removed from the cracked mortar samples, and the crack feature of each mortar sample was examined. To examine cracks, a photo was taken from each end of a cracked sample using a camera (see image on the left in Figure 13). The file of the photo was then inputted into the CAD software, or computer-aided design and drafting (CADD), computer program, which highlighted the crack features and computed crack area and crack widths (see image on the right in Figure 13).



**Figure 13. Crack in a mortar sample captured by camera (left) and crack retrieved by CAD software (right)**

Figure 14 illustrates the cross sections of the 20 cracked mortar samples, and Figure 15 highlights the features of the cracks captured by CAD for the samples listed in Figure 14.

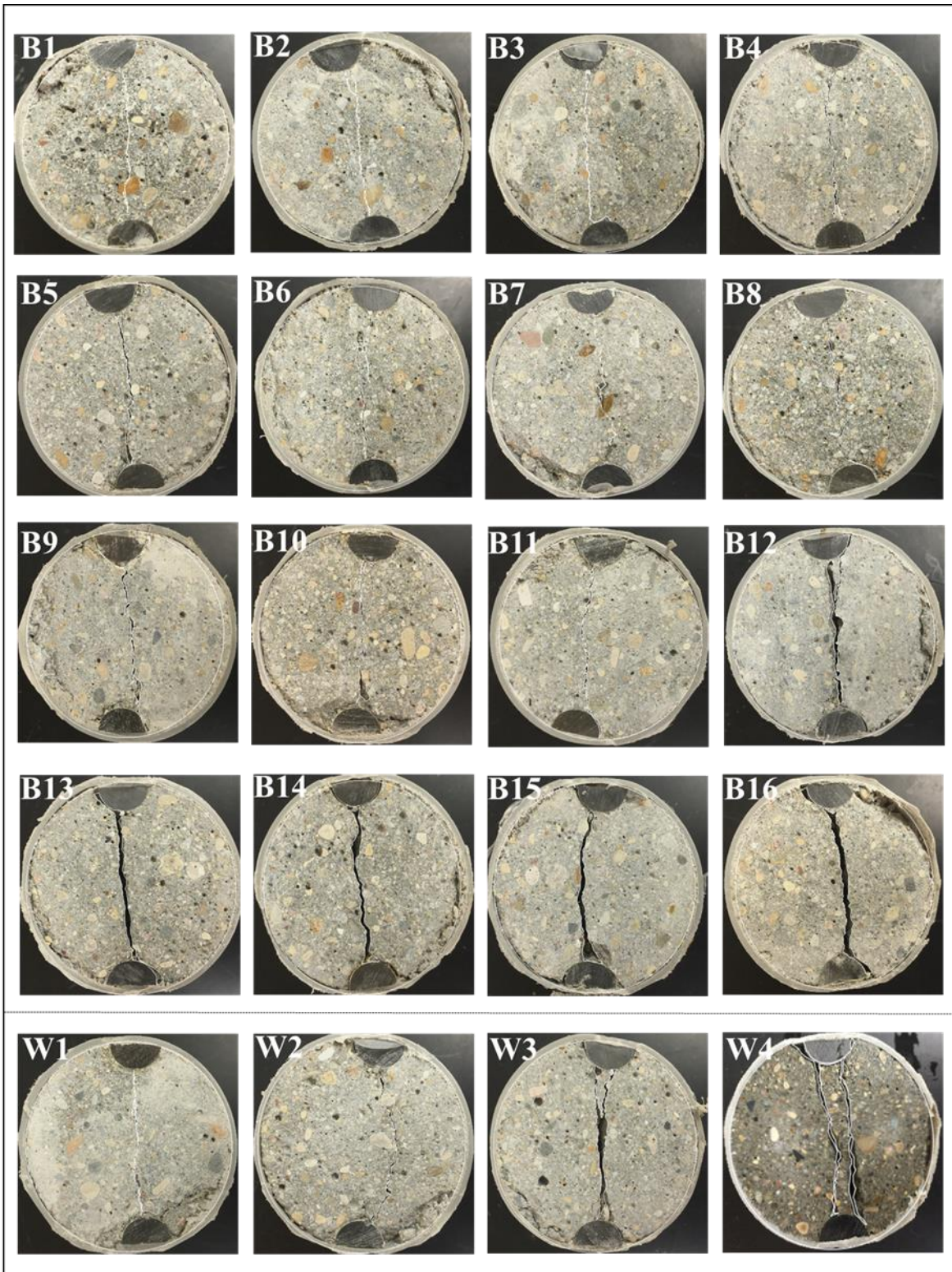


**Figure 14. Top surface of mortar samples with different crack sizes**

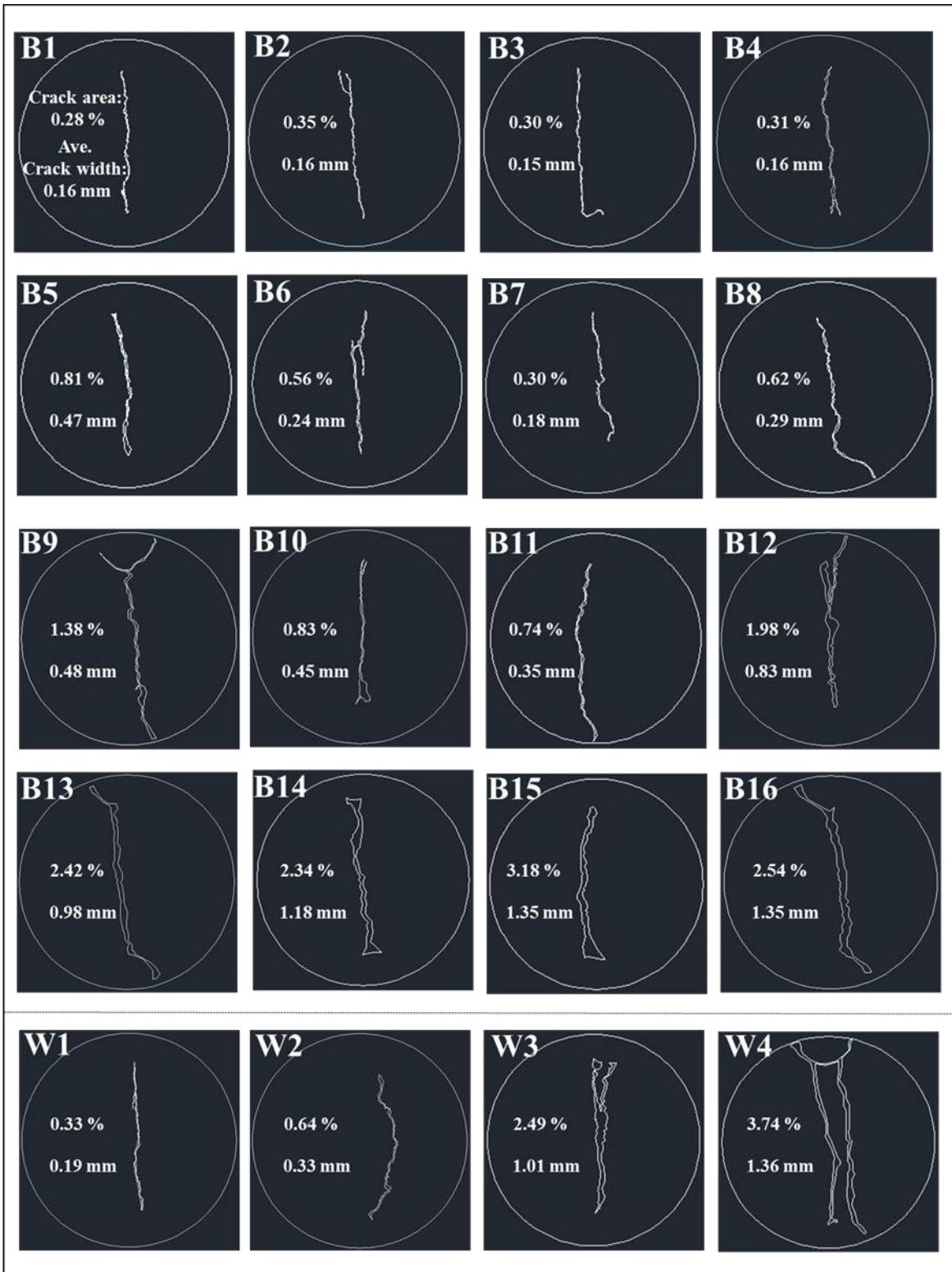


Figure 15. Top surface of mortar samples with different crack sizes captured by CAD software

In Figure 15, the crack area was expressed as a percentage of the total cross-section area of a sample:

$$\text{Crack area (\%)} = (\text{crack area} / \text{sample cross section area}) \times 100\% \quad (1)$$

Considering that the crack width and length at one end of a particular mortar sample was slightly different from the crack at the other end, the crack size of each sample was defined as the average crack size of the two ends of each cracked mortar cylinder sample studied. The average of crack width (mm) of a sample was calculated by its average crack area divided by crack length.

$$\text{Crack width (mm)} = \text{average crack area (mm}^2\text{)} \div \text{average crack length (mm)} \quad (2)$$

Among the 20 cracked mortar samples, 16 samples with different crack sizes were used for biogROUT repair tests or treated with biogROUT solutions, and 4 samples, also with different crack sizes, were used for a comparison test or soaked in water only.

#### 5.1.5 Crack Repair

Two types of solutions were prepared for crack repair of the above-mentioned 16 mortar samples: one was the UPB solution and the other was the urea-CaCl<sub>2</sub> solution (as described previously). The following procedures were used for the repair:

1. Soak each cracked sample in a 60 ml of UPB solution in a plastic cup for 2 hours and allow the samples to saturate.
2. Place the samples on a table for 5 minutes and let the UPB solution drain.
3. Soak all the samples in a container with 4 liters of the urea-CaCl<sub>2</sub> solution for approximately 22 hours using a stir bar and plate to keep the solution circulating.
4. Place the samples on the table for 5 minutes again.
5. Repeat steps 1 through 4.

The above steps 1 through 4 were considered as one cycle treatment, which took one day to complete. See Figure 16 for a visual representation of the entire process.

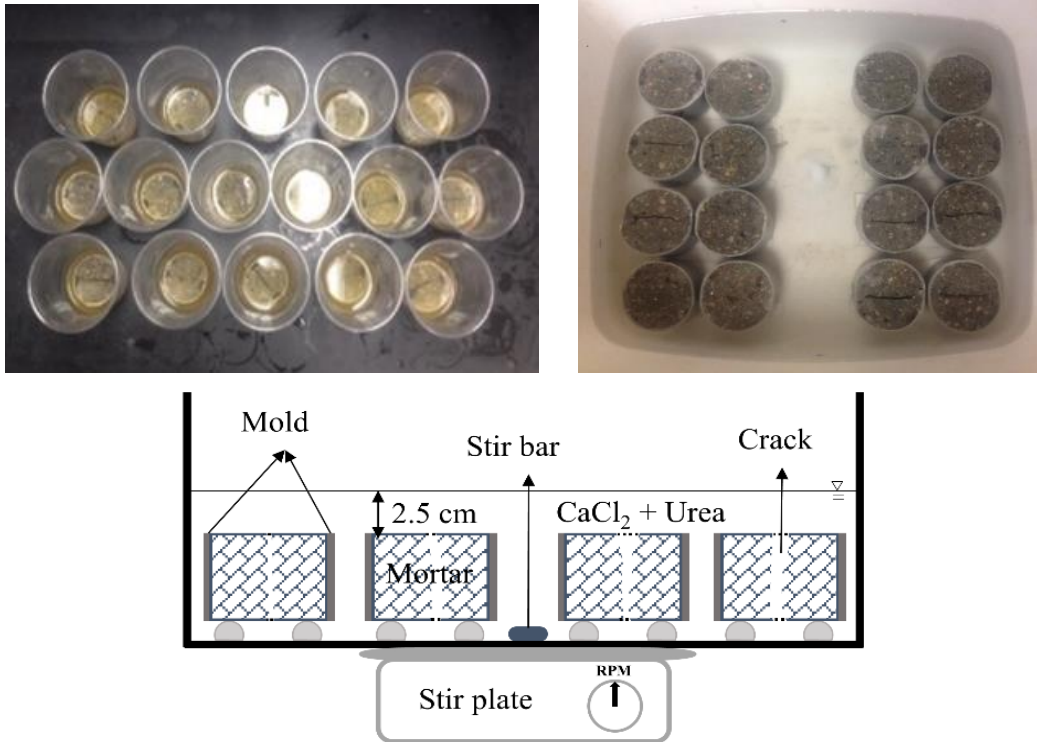


**Figure 16. Process of crack repair using the MICP method: Samples in UPB solution (upper left), samples in urea-CaCl<sub>2</sub> solution (upper right), and process sketch (bottom)**

## 5.2 Test and Methods

To evaluate the effectiveness of the crack repair method, permeability of the cracked mortar samples was tested at 0, 7, 14, and 21 cycles of the MICP treatment. TS of the samples was measured after the permeability test at 21 cycles. The split surfaces of these sample were then examined, and the amount of CaCO<sub>3</sub> was estimated and expressed as the percentage of the area covered by CaCO<sub>3</sub> to the total cross-section area of the sample.

### 5.2.1 Water Permeability

Water permeability of the repaired samples was measured at every 7th cycle of treatment (i.e., 7, 14, 21 cycles). To conduct the water permeability test, samples were first soaked in water a day before the permeability test. After one day, 20 samples were measured using a constant head permeability test according to ASTM D 2434-68.

### 5.2.2 Splitting Tensile Strength

After the final permeability tests, samples were taken out of the biocement solutions and placed on a table to dry under a lab environment of about 23°C and 50% RH for two days. After 2 days, 16 of the samples (B1 to B16) were tested for TS according to ASTM C 496. In the test, splitting

loads were applied to the repaired samples at their crack locations, thus evaluating the bond/adhesion strength provided by the biogROUT to the cracked mortar.

### 5.2.3 Calcium Carbonate Content

After TS tests, the surfaces of the broken samples were examined for CaCO<sub>3</sub> content. To estimate the CaCO<sub>3</sub> content, a grid was applied onto the surface of an examined sample. The surface areas that were covered by precipitated CaCO<sub>3</sub> were assessed. The CaCO<sub>3</sub> content was expressed as the percentage of the surface areas that were covered by precipitated CaCO<sub>3</sub> to the total surface area of the sample examined. For each cracked mortar sample, the CaCO<sub>3</sub> content was determined by the average value obtained from its two cracked surfaces.

## 5.3 Results and Discussion

Table 6 summarizes the water permeability, TS, and precipitated CaCO<sub>3</sub> content of all cracked mortar samples tested, where samples B1 through B16 were repaired using MICP solutions and samples W1 through W4 were soaked in distilled water. Note that the sample ID is arranged based on the order of the average crack width (from smallest to largest).

**Table 6. Crack sizes and test results of all cracked mortar samples studied**

ID	Initial Crack		Water Permeability (m/sec)				CaCO <sub>3</sub> content (%) at 21 cycles	Tensile strength (kPa) at 21 cycles
	Avg. width (mm)	Crack area (%)	0 cycles	7 cycles	14 cycles	21 cycles		
B1	0.15	0.26	9.237E-6	2.777E-6	2.616E-6	2.257E-6	5.3	46
B2	0.17	0.49	6.953E-5	7.229E-6	2.046E-6	1.068E-6	5.9	32
B3	0.19	0.36	6.647E-5	8.873E-6	5.015E-6	4.829E-6	3.1	355
B4	0.22	0.39	6.938E-5	4.055E-6	1.444E-6	9.212E-7	3.2	61
B5	0.23	0.45	1.587E-5	5.700E-6	3.109E-6	9.046E-7	4.2	290
B6	0.24	0.69	1.117E-4	8.408E-6	1.417E-6	9.189E-7	7.8	162
B7	0.27	0.49	1.344E-4	1.157E-5	3.034E-6	2.497E-6	3.6	296
B8	0.33	0.63	1.799E-4	9.694E-6	2.701E-6	1.718E-6	19.4	381
B9	0.39	1.16	2.338E-4	7.792E-6	1.425E-6	1.243E-6	6.6	111
B10	0.52	0.94	1.471E-4	1.008E-5	3.262E-6	2.479E-6	7.2	193
B11	0.62	1.50	4.443E-4	6.390E-6	5.419E-6	4.294E-6	20.4	126
B12	0.74	1.82	1.013E-3	2.452E-5	7.819E-6	2.456E-6	54.6	136
B13	1.04	2.52	1.902E-3	5.707E-5	1.464E-5	9.650E-6	77.2	281
B14	1.09	2.18	1.116E-3	5.994E-5	1.909E-5	4.847E-6	80.5	386
B15	1.37	3.20	3.027E-3	8.254E-5	2.287E-5	4.947E-6	64.8	115
B16	1.64	3.28	1.722E-3	6.619E-5	6.976E-6	3.978E-6	69.4	143
W1	0.17	0.30	1.119E-5	6.895E-6	6.782E-6	6.731E-6	0	0
W2	0.31	0.61	2.054E-4	1.570E-4	1.615E-4	1.563E-4	0	0
W3	0.85	2.04	4.603E-4	3.600E-4	3.550E-4	3.471E-4	0	0
W4	1.72	3.78	2.333E-3	2.193E-3	2.135E-3	2.044E-3	0	0

B in sample ID denotes an MICP treatment; W denotes a water treatment

Figure 17 shows a strong linear relationship between the crack width and area of the repaired samples. Therefore, the average crack width was used as the representative crack size for the data analysis of the present study.

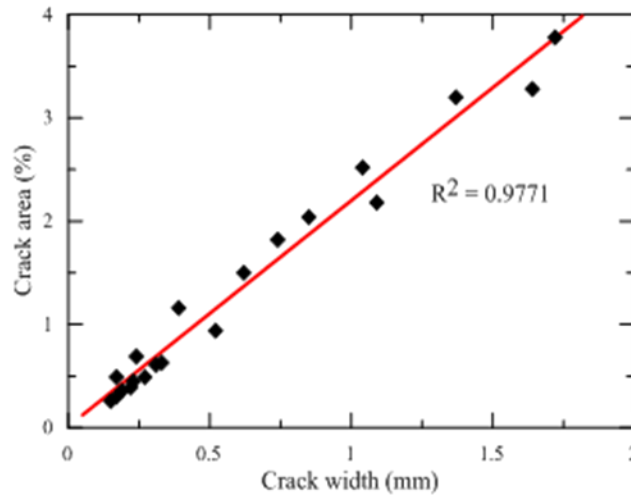


**Figure 17. Relationship between the crack width and crack area of mortar samples**

### 5.3.1 Crack Healing

Figure 18 shows the top surfaces of the cracked cylinder mortar samples after they were subjected to 7, 14, and 21 cycles of MICP/water treatment. It can be seen from the figure that, for the MICP-treated samples, cracks gradually healed with the increasing number of treatment cycles. After 7 cycles, most small cracks were healed, and after 21 cycles all cracks were healed. It should be noted that not only were the cracks filled with the precipitated  $\text{CaCO}_3$  resulting from the MICP process, but the entire cross sections of the repaired samples were also covered. However, microscopic study of the internal crack surfaces of the split samples, as discussed later, indicated that there were 1/16 to 1/8 inches of precipitated  $\text{CaCO}_3$  layers covered each end of the cylinder samples, but the internal crack surfaces were not 100% covered with precipitated  $\text{CaCO}_3$ .

Differently, there was little significant crack healing in samples soaked in distilled water. The surfaces of these water treated mortar samples showed clearly the cement paste and sand particles.

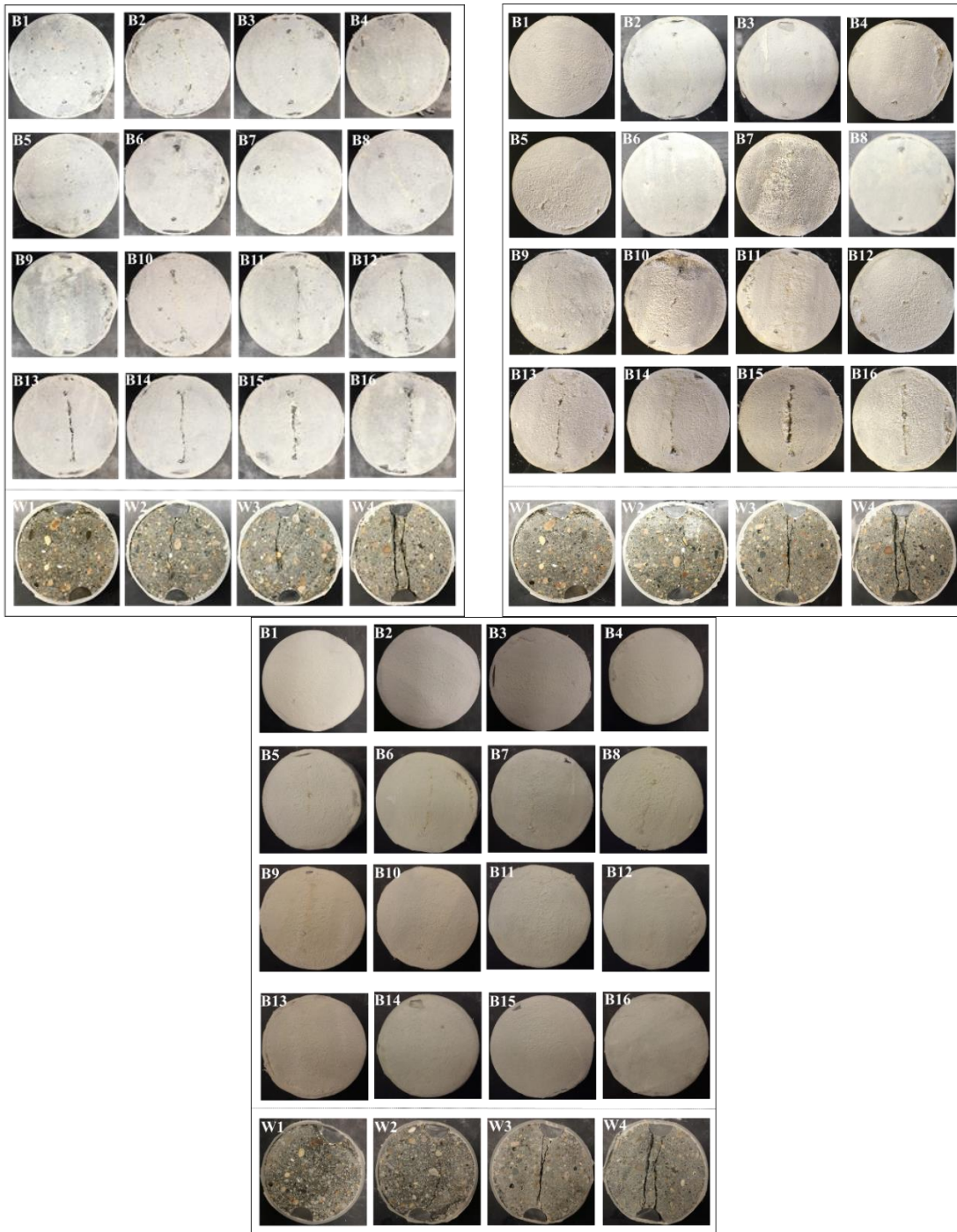


**Figure 18. Cracks in mortar samples after 7 cycles (left), 14 cycles (right), and 21 cycles (bottom) of MICP treatment**

### 5.3.2 Permeability

Figure 19 illustrates water permeability of cracked mortar samples subjected to different cycles of MICP and water treatment.

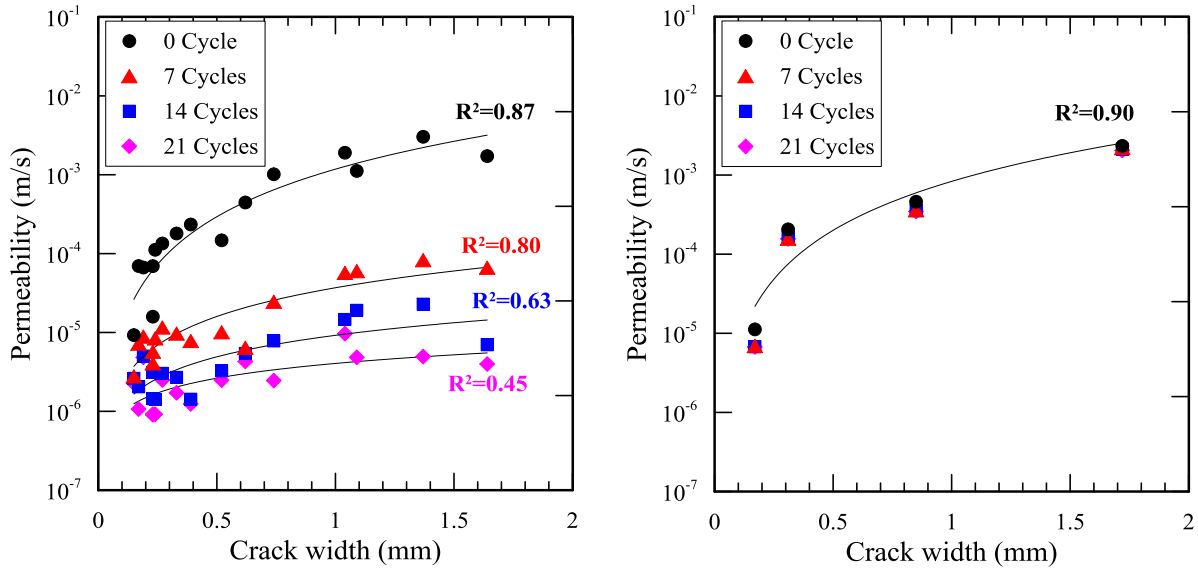


**Figure 19. Effect of initial crack size on permeability of mortar samples after MICP treatment (left) and water treatment (right)**

The graph on the left generally shows permeability of the mortar samples polynomial increased with their average crack widths. As the initial crack width was about 2 mm, the mortar without treatment had a permeability value of about  $8.0E-5$ , which is consistent with measurements by other researchers (Wang et al. 1997 and Van Tittelboom et al. 2010).

Before any treatment, the cracked mortar samples, with a crack size ranging from 0.15 to 1.64 mm (average of 0.58 mm), had permeability values ranging from  $3.027E-3$  to  $9.237E-6$  m/s (average of  $6.413E-4$  m/s). After treated with MICP for 7 cycles, their permeability decreased to the range of  $8.254E-5$  to  $2.046E-6$  m/s (average of  $2.330E-5$  m/s), which was almost 28 times lower. The permeability values continuously decreased with the number of treatment cycles. After being treated with MICP for 21 cycles, the permeability of the mortar samples was only around  $1.000E-6$  m/s or less.

The graph on the left in Figure 19 also shows the R-squared values of the fitted regression curves. For samples with no treatment, the permeability curve had a high R-squared value (0.87). As the number of treatment cycles increased, the R-squared value of the permeability measurements of the samples decreased. The reduced R-squared value might be attributed to the amount and size of precipitated  $\text{CaCO}_3$  in the cracks of the samples. After a certain level of MICP treatment, it is not the initial cracks but the microstructure of biocement (network of  $\text{CaCO}_3$ ) in the cracks that might control the permeability of the samples. Al Qabany et al. (2013) reported that the small size of  $\text{CaCO}_3$  could be produced from a strong biocementation using *bicillus sp.* at a low chemical concentration (urea- $\text{CaCl}_2$ ).

The graph on the right in Figure 19 shows the permeability changes in samples treated with distilled water. It can be noticed that the permeability of samples at 0 cycles (no treatment) was slightly higher than that of samples treated with water. For samples with small average crack

widths ( $\leq 0.2$  mm), permeability decreased noticeably (almost by 1.6 after 7 cycles of water treatment), while for samples with larger average crack widths (1.8 mm), the decrease in permeability was barely visible. This implied that the mortar samples had autogenous crack healing under water treatment, which was provided by cement hydration (Barneyback and Diamond 1981). Such autogenous crack healing was more effective for samples with small cracks ( $\leq 0.2$  mm) and much less effective for samples with larger cracks ( $> 0.2$  mm). After 7 cycles of water treatment, permeability of the samples did not reduce further.

Figure 20 shows the effect of treatment time (in cycles) on the permeability of each sample studied.

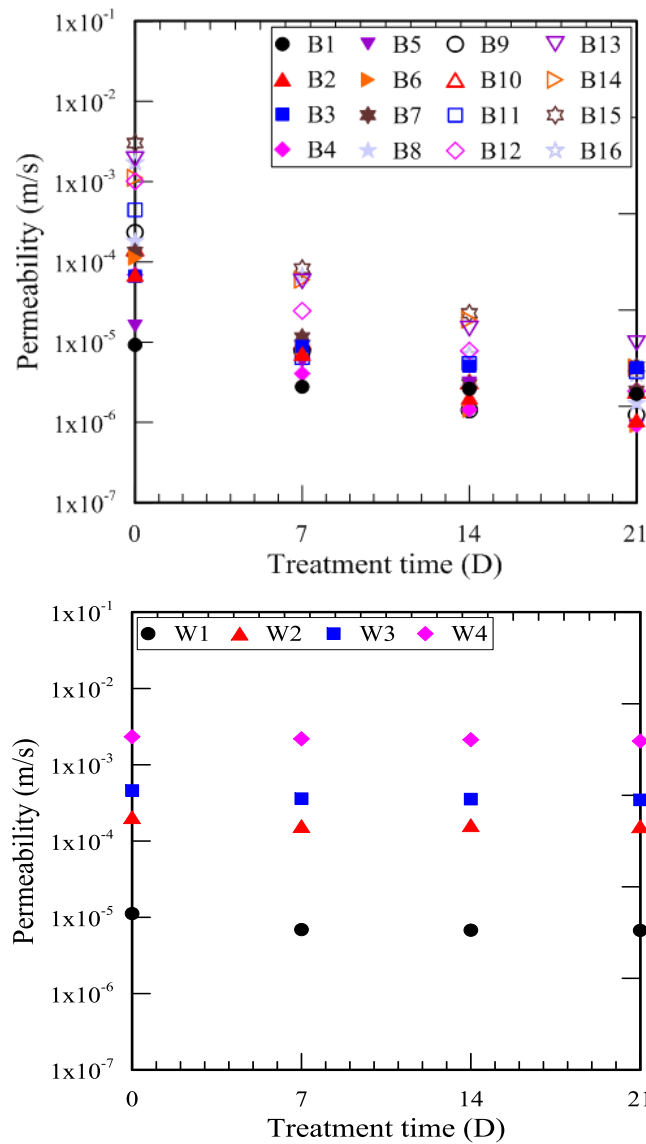


**Figure 20. Relationship between permeability and cycles time during MICP treatment (top) and water treatment (bottom)**

For samples treated with MICP, permeability significantly decreased with the number of treatment cycles. The permeability decreased more rapidly during the first 7 cycles and then decreased relatively slowly. The permeability of samples with large cracks tended to decrease more rapidly than that of samples with small cracks. As discussed previously, the permeability of the sample treated with water had little change during the first 7 cycles and kept unchanged further after.

### 5.3.3 Splitting Tensile Strength

Splitting tensile strength was performed on the samples treated with MICP (samples B1 to B16) after 21 cycles, but TS tests were not performed for samples treated with water (samples W1 to W4) because these samples were broken into two pieces after their plastic molds were removed. That is, autogenous crack healing provided by cement hydration didn't provide enough of a significant bond to hold the samples together.

Figure 21 shows the stress-strain curve obtained from TS tests of the MICP treated samples with different crack widths.

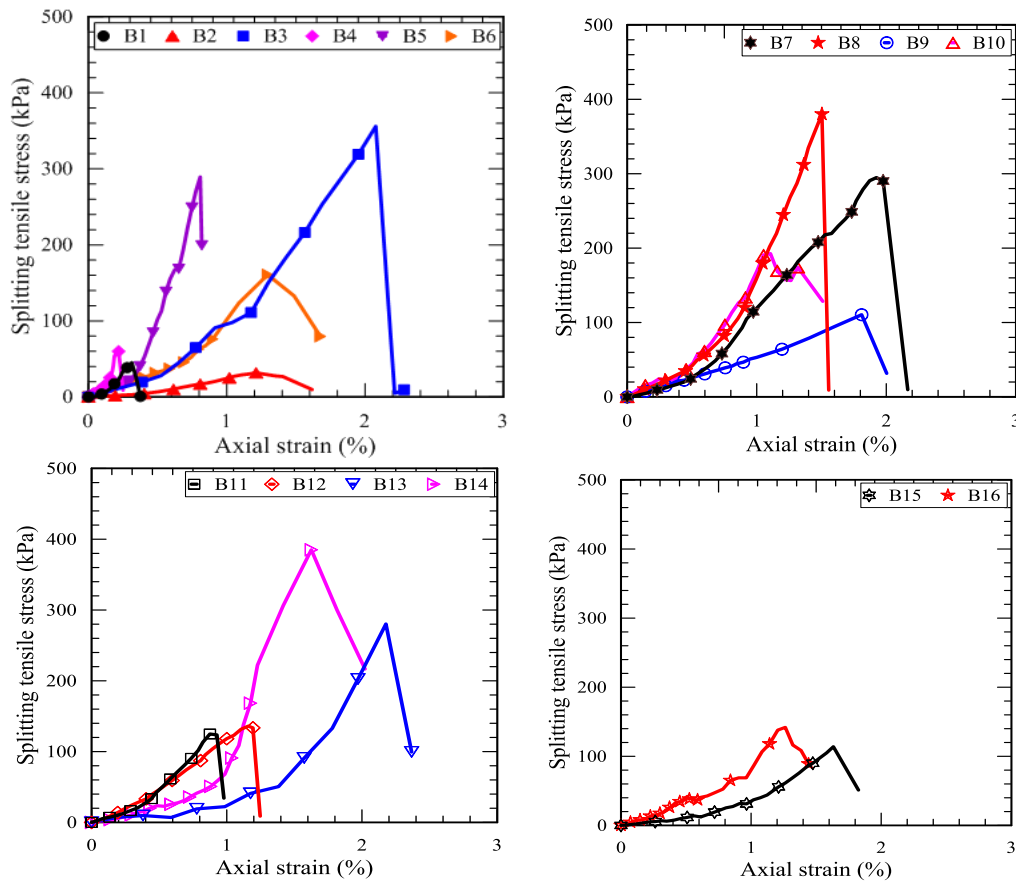


**Figure 21. Splitting stress-strain curves of repaired samples with different crack sizes: average crack width < 0.25 mm (top left), average crack width = 0.25-0.52 mm (top right), average crack width = 0.62-1.09 mm (bottom left), and average crack width > 1.09 mm**

The following observations were made:

1. TS of the repaired samples ranged from 32 to 386 kPa. Among all 16 samples tested, 3 samples (B1, B2, and B4) had a TS less than 100 kPa, 7 samples had a TS between 111 and 193 kPa, 3 samples (B5, B7, and B13) had a TS between 281 to 296 kPa, and 3 samples (B3, B8, and B14) had a TS between 355 and 386 kPa.
2. The maximum strain of the samples ranged from 0.22 to 2.17%. Among all 16 samples tested, only samples B1 and B4 had a maximum strain less than 0.4%, while most samples had a maximum strain larger than 1.0% compared to 0.3% for most intact conventional concrete/mortars.
3. Most repaired samples showed linear stress-strain behavior, indicating potential brittleness of the precipitated  $\text{CaCO}_3$ .

Figure 22 shows the relationship between crack width and precipitated  $\text{CaCO}_3$  content on the crack surface.

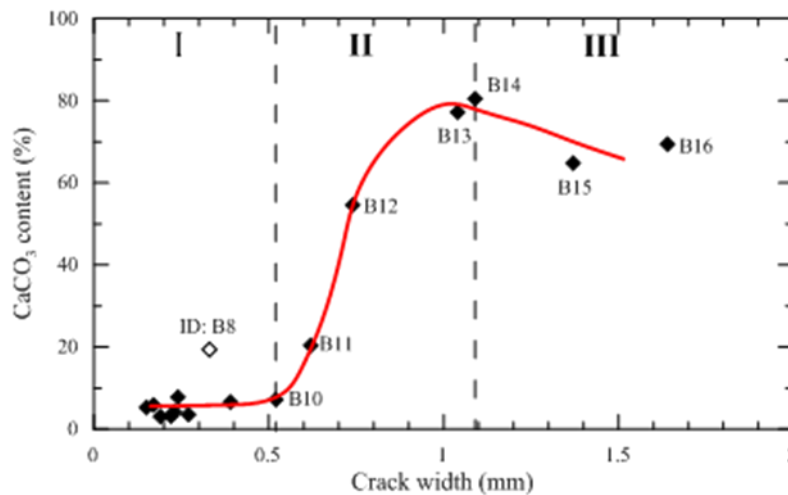


**Figure 22. Relationship between crack width and precipitated  $\text{CaCO}_3$  content**

In Region I (average crack width  $<0.52$  mm),  $\text{CaCO}_3$  content on the crack surface was very low and fluctuated around 5% (varying from 3.2 to 7.8%). This suggested that only a small amount of the chemical and bacteria solutions got into those small cracks and performed the MICP process there. In Region II ( $0.52$  mm  $\leq$  average crack width  $\leq 1.1$  mm),  $\text{CaCO}_3$  content on the crack surface increased with the crack width (up to approximately 80%). This indicated that MICP was more effective for cracks within this size range. In Region III (average crack width  $>1.1$  mm),  $\text{CaCO}_3$  content on the crack surface started decreasing slightly with the crack width.

Figure 23 shows the relationship between TS and precipitated  $\text{CaCO}_3$  content/initial average crack width.

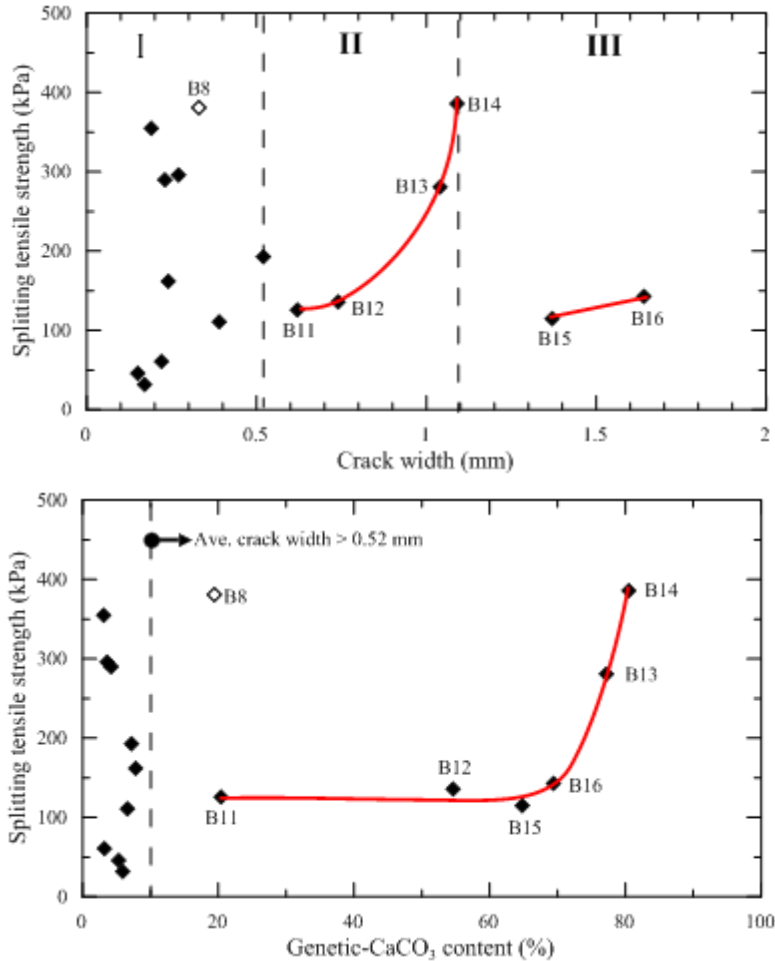


**Figure 23. Relationship between tensile strength and CaCO<sub>3</sub> content (top) and initial average crack width (bottom)**

The top graph in Figure 23 shows that in the small crack region (Region I), some samples regain relatively high TS (up to 386 kPa) while others had very low TS (32 kPa) after the MICP repair. This might happen for several reasons: (1) some samples might not split totally, and their uncracked portion might carry some loads during the splitting tests; (2) since the crack widths of the samples were very small, or their two cracked surfaces are close together, a little precipitated CaCO<sub>3</sub> in the cracks might generate a high adhesion on the cracked surfaces, which helped the splitting resistance; and (3) after a few MICP cycles, the precipitated CaCO<sub>3</sub> quickly sealed the small crack on the top of the cylinder samples and prevented UPB and urea/CaCl<sub>2</sub> solutions from easily penetrating into the internal cracks, thus increasing the variation in the effectiveness of the MICP repair, which resulted in inconsistent TS test results. In the large crack region (Region III), the TS of the MICP-repaired samples were relatively low, probably due to the insufficient CaCO<sub>3</sub> bridging the cracks. It appeared that MICP was more efficient for repair of mortar cracks with a size ranging from 0.5 to 1.1 mm (Region II).

The bottom graph in Figure 23 shows that there was no clear relationship between TS and the CaCO<sub>3</sub> content since the sample average crack width was  $\leq 0.5$  mm. As a note, sample B8 had an

average crack width of 0.33 mm. However, a clear relationship was observed, because the sample average crack width was  $>0.52$  mm while the TS increased with  $\text{CaCO}_3$  content.

### 5.3.4 Microstructure Study

After the TS tests, the samples were examined under a SEM, and the distribution and morphology of the precipitated  $\text{CaCO}_3$  on the surfaces of the sample cracks were observed. Figure 24 shows images of one sample surface (ID B14).

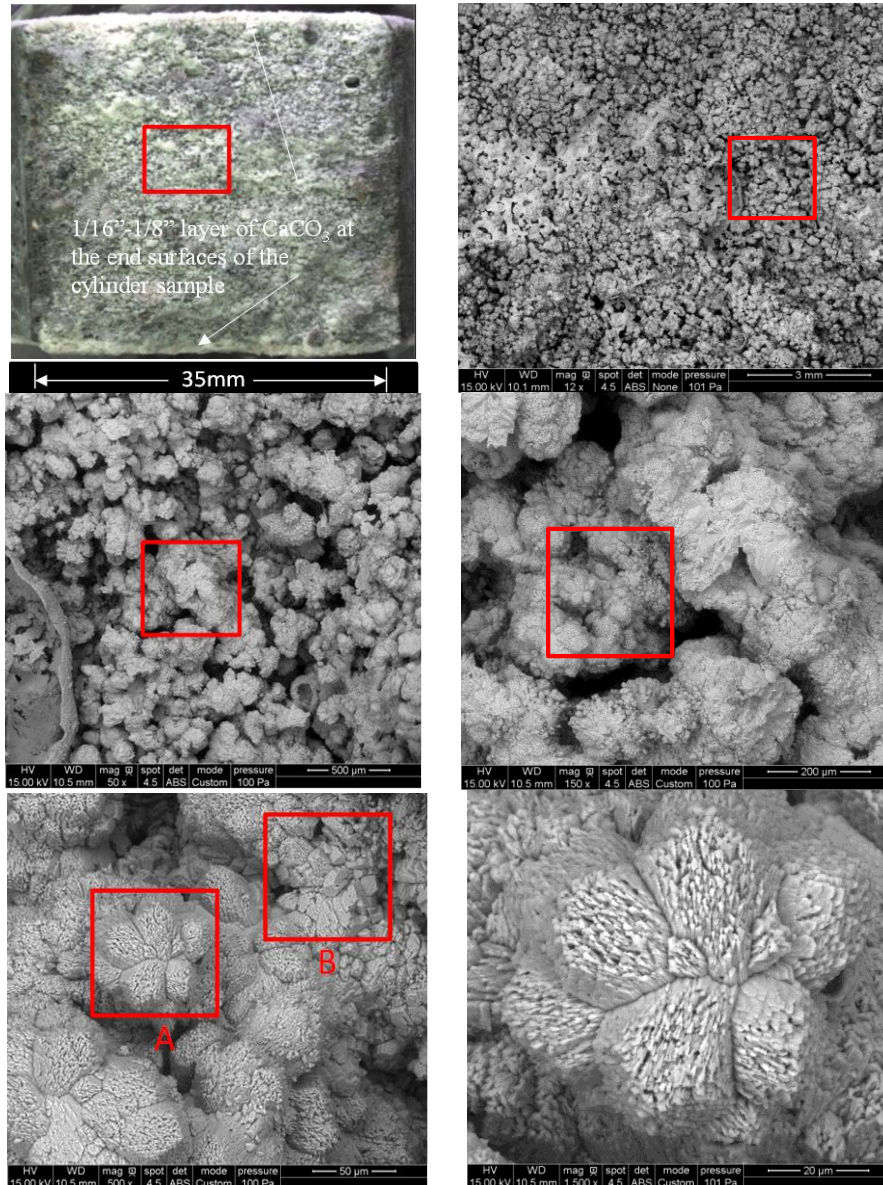


**Figure 24. Precipitated  $\text{CaCO}_3$  on the cracked surface of mortar sample B14: crack surface of the split sample (top left), 12X magnification of the crack surface (top right), 50X magnification (middle left), 150X magnification (middle right), 500X magnification (bottom left), and 1,500X magnification (bottom right)**

The top left image in Figure 24 shows that after being subjected to the MICP treatment for 21 cycles, the end surfaces of the cylinder sample were covered with a 1/16 in. to 1/8 in. layer of precipitated  $\text{CaCO}_3$ , which might have served as the front line for resisting water penetration. However, the top right and middle left images in Figure 24 show the growth and distribution of precipitated  $\text{CaCO}_3$  on the cracked mortar surface. It appeared that precipitated  $\text{CaCO}_3$  was relatively uniformly distributed on the crack surfaces, and it formed a porous matrix at a microscale. The middle right, bottom left, and bottom right images in Figure 24 show the structure and texture of the precipitated  $\text{CaCO}_3$ . It can be observed in Figure 13 that there were two different  $\text{CaCO}_3$  formations in the crack of sample B14: one was the flower-shaped clusters made with many well-arranged thin (or plate/sheet-like) hexagon  $\text{CaCO}_3$  and the other was the granular clusters of thick (or coarse) hexagon-shaped  $\text{CaCO}_3$  at multiple scales, which was also observed in the cracks of other MICP-repaired mortar samples (see Figure 25).

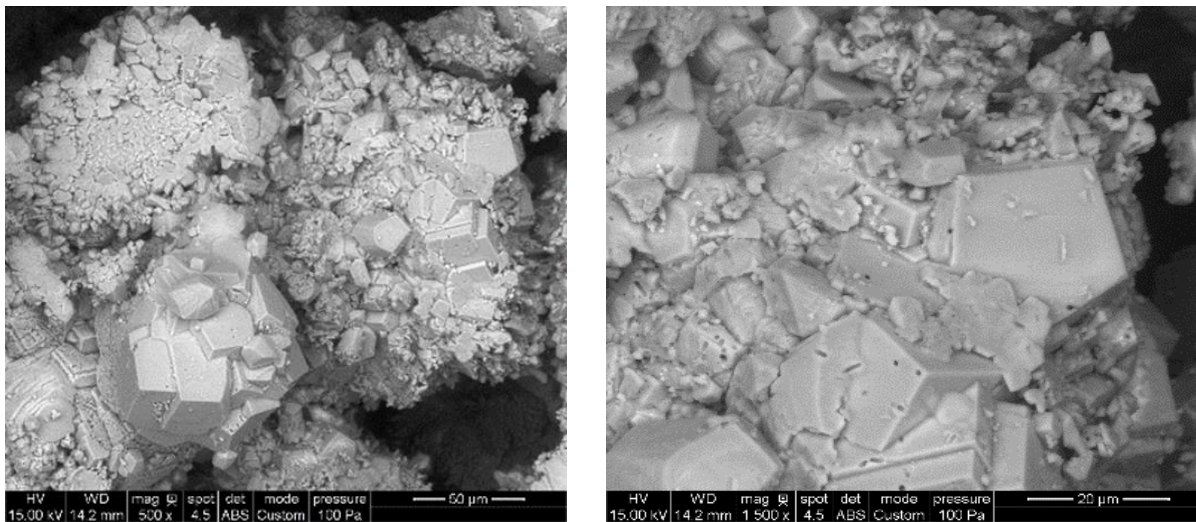


**Figure 25. Coarse hexagon-shaped  $\text{CaCO}_3$  observed on the cracked surface of sample B15 at 500 times the actual size (left) and at 1,500 times the actual size (right)**

Research has indicated that the precipitated material during a MICP process involving UPB and  $\text{CaCl}_2$  solutions are often coarse hexagon-shaped  $\text{CaCO}_3$ , or calcite (Abo-El-Enein et al. 2012 and Choi et al. 2016b), which is a thermodynamically stable form of  $\text{CaCO}_3$  under normal conditions. Generally, a smaller size (less than  $10\ \mu\text{m}$ ) of calcite provides better strength for the biocemented materials (Choi et al. 2016b). In the present study, the precipitated  $\text{CaCO}_3$  was also in a calcite form and had a size ranging from  $5$  to  $20\ \mu\text{m}$ , which was similar to samples observed by Al Qabany and Soga (2013). The sheet-like, thin hexagon-shaped  $\text{CaCO}_3$ , as observed in Figure 24 might be vaterite. Vaterite is a metastable phase of  $\text{CaCO}_3$ , and it might convert to calcite after being exposed to water. Further study is needed to find out why different forms of  $\text{CaCO}_3$  were observed in a given sample.

#### 5.4 Summary

Cracks with various sizes ( $0.15$  to  $1.72\ \text{mm}$  in average width) were generated in 20 cylindrical mortar samples using a splitting tensile test. Four of the cracked samples were soaked in distilled

water, and 16 were repaired using the MICP technology. Two solutions were used in the MICP repair: (1) a UPB solution made with *bacillus sp.*, which was cultured in a medium made of a yeast extract (20 g), ammonium sulfate, and a 0.13 M Tris buffer (pH=9.0) solution; and a (2) 0.2 M urea-CaCl<sub>2</sub> solution. The results indicated that the cracks in the samples treated with distilled water did not heal up to 21 days, while the cracks in the samples treated with MICP solutions gradually healed with an increasing number of MICP treatment cycles. The samples treated with MICP had a significant reduction in water permeability. While water-treated samples were too weak to test, the MICP-treated samples had a TS ranging from 32 to 386 kPa after 21 treatment cycles. For the samples with an initial average crack width of >0.52 mm, the TS clearly increased with the CaCO<sub>3</sub> content resulting from the MICP treatment. A SEM study suggested that there were two different forms of CaCO<sub>3</sub> on the crack surface of cracked mortar samples: one was vaterite and the other calcite. The CaCO<sub>3</sub> crystals had a size ranging from 5 to 20 μm, and they formed a porous matrix that filled in the mortar cracks.

## 6 CONCLUSIONS AND RECOMMENDATIONS

The study's goal was to develop an eco-friendly, cost-effective biocement/grout for sand cementation and mortar crack repair. It included two main parts: development of a new soluble calcium solution for MICP using industrial and agricultural by-products and study of mortar crack repair using MICP technology.

The following conclusions can be drawn concerning the development of a new soluble calcium solution for MICP:

- The soluble calcium solution for MICP can be achieved from dissolving a limestone powder (an industrial by-product from a limestone quarry) into an acetic acid-rich SF5 solution, which is derived from a pyrolysis and bio-oil fractionation system; the pyrolysis feedstock was a mix of softwood including pine, aspen, poplar, birch, and maple.
- The properties of the soluble calcium solution for MICP can be optimized from the study of different limestone powder-to-SF5 ratios, pH values of the obtained solutions, and procedures for applying the UPB and media (urea/calcium solutions) for CaCO<sub>3</sub> precipitation (MICP treatment). The optimal 0.3 M calcium solution obtained from the present study consists of a limestone:SF5:NaOH:distilled water ratio of 1:8:0.045:13 (by weight). Using such a soluble calcium solution made with industrial and waste by-products to replace for CaCl<sub>2</sub> in a MICP process has provided desirable CaCO<sub>3</sub> precipitation.
- The properties of the sand samples biocemented using the newly developed soluble calcium solution are comparable to those of the sand samples biocemented using CaCl<sub>2</sub> as a calcium source for MICP. The CaCO<sub>3</sub> content of the sand samples biocemented using the new calcium source ranged from 5.67 to 8.19%. The permeability of the biocemented sand ranged from 8.17E-6 to 1.52E-6 m/s, UCS ranged from 858 to 1,111 kPa, TS ranged from 137 to 197 kPa, UCS/TS ratios ranged from 4.6 to 6.9, and the E<sub>50</sub> is 38.3±1.7 MPa for compression and 24.3±2.7 MPa for tension.
- There are close relationships between the engineering properties (permeability, UCS, TS, UCS/TS ratio, and E<sub>50</sub>) of the biocemented sand samples and the CaCO<sub>3</sub> content in the samples. Generally, the permeability decreases and strength and modulus of elasticity increases with increasing CaCO<sub>3</sub> content.

The following conclusions can be drawn concerning the study of mortar crack repair using MICP technology:

- Cracks in the mortar samples repaired using the MICP technology gradually healed with an increasing number of treatment cycles. After 7 cycles, most small cracks (<0.52 mm) were healed. After 21 cycles, all cracks (0.15 to 1.64 mm) were healed with 1/16 to 1/8 in. of precipitated CaCO<sub>3</sub> layers on the top surfaces of repaired cylinders. Differently, for samples treated with distilled water only, there was little visible crack healing after 21 cycles.

- For samples with an average crack width  $<0.52$  mm,  $\text{CaCO}_3$  content on the crack surface was very low, varying from 3.2 to 7.8%, indicating that the UPB and urea/ $\text{CaCl}_2$  solution might have had some difficulties getting into the fine cracks and performing the MICP process there. For samples with an average crack width between 0.52 mm and 1.1 mm,  $\text{CaCO}_3$  content on the crack surface increased with the crack width (up to approximately 80%). This indicates that MICP was more effective for cracks within this size range. For samples with an average crack width  $>1.1$  mm,  $\text{CaCO}_3$  content on the crack surface started decreasing slightly with the crack width.
- The MICP repair technique can significantly reduce water permeability of cracked samples. Before any MICP treatment, the cracked mortar samples, with crack sizes ranging from 0.15 to 1.64 mm, had permeability values ranging from  $3.027\text{E-}3$  to  $9.237\text{E-}6$  m/s. After being treated with MICP for 7 cycles, their permeability decreased to the range of  $8.254\text{E-}5$  to  $2.046\text{E-}6$  m/s. After being treated with MICP for 21 cycles, the permeability of the mortar samples was only around  $1.000\text{E-}6$  m/s or less.
- For samples with small average crack widths ( $\leq 0.2$  mm), permeability decreased noticeably after 7 days of water treatment, while for samples with large average crack widths (e.g., 1.8 mm), the decrease in permeability was barely measured, and permeability of the samples did not reduce further with the increasing number of water treatment cycles. That is, autogenous crack healing resulting from cement hydration under water was more effective for samples with small cracks ( $\leq 0.2$  mm) and much less effective for samples with larger cracks ( $>0.2$  mm).
- The TS of the MICP-repaired samples ranged from 32 to 386 kPa, and the maximum strain of the samples ranged from 0.22 to 2.17% after 21 treatment cycles. Most of the samples (except for B1 and B4) had a maximum strain larger than 1.0%, compared to 0.3% for most intact conventional concrete/mortars and their stress-strain behavior was generally linear. However, the water treated mortar samples were all broken into two pieces after demolding, and therefore they were unable to be tested for TS.
- There was no clear relationship between TS and the  $\text{CaCO}_3$  content, because the samples had an average crack width of  $\leq 0.5$  mm. However, a clear relationship was observed for the sample average crack widths  $>0.52$  mm, where TS increased with  $\text{CaCO}_3$  content.
- The SEM study suggested that there were two different forms of  $\text{CaCO}_3$  in the cracked mortar samples: one form consisted of flower-shaped clusters made with well-arranged thin (plate/sheet-like) hexagon  $\text{CaCO}_3$ , which might be vaterite, and the other was the granular clusters made with thick (coarse) hexagon  $\text{CaCO}_3$ , which was probably calcite. The  $\text{CaCO}_3$  crystals had a size ranging from 5 to 20  $\mu\text{m}$ , and they formed a porous matrix that filled in the cracks.

The following recommendations are proposed for further study:

- In this study, the limestone powders and the acetic acid-rich SF5 solution were obtained from given sources. The properties of these raw materials from different sources may vary. The effects of the variations in the raw materials on the properties of the resulting soluble calcium solution should be further studied.
- In addition to soaking, different treatment methods (e.g., injection and spraying) should be investigated, as they are commonly used repair methods in constructions.
- An in-depth study should be conducted to find out why different forms of  $\text{CaCO}_3$  (calcite and vaterite) were observed in a given sample.

## REFERENCES

- Abo-El-Enein, S. A., Ali, A., H., Talkhan, F. N. and Abdel-Gawwad, H. A. 2012. Utilization of microbial induced calcite precipitation for sand consolidation and mortar crack remediation. *Housing and Building National Research Center*, Vol. 8, pp. 185–192.
- Achal, V., Mukerjee, A., and Reddy, M. S. 2013. Biogenic treatment improves the durability and remediates the cracks of concrete structures. *Construction and Building Materials*, Vol. 48, pp. 1–5.
- Al Qabany, A. and Soga, K. 2013. Effect of chemical treatment used in MICP on engineering properties of cemented soils. *Géotechnique*, 63(4): 331–339.
- Barneyback, R. S. and Diamond, S. 1981. Expression and analysis of pore fluids from hardened cement pastes and mortars. *Cement and Concrete Research*, 11(2): 279–285.
- Choi, S. G., Wu, S., and Chu, J. 2016a. Biocementation for Sand Using an Eggshell as Calcium Source. *Journal of Geotechnical and Geoenvironmental Engineering*, Vol. 142, No. 10.
- Choi, S. G., Wang, K., and Chu, J. 2016b. Properties of Biocemented, Fiber Reinforced Sand. *Construction and Building Materials*, Vol. 120, pp. 623–629.
- Chu, J., Ivanov, V., Stabnikov, V., and Li, B. 2013. Microbial method for construction of an aquaculture pond in sand. *Géotechnique*, 63(10): 871–875.
- Chu, J., Stabnikov, V., and Ivanov, V. 2012. Microbially induced calcium carbonate precipitation on surface or in the bulk of soil. *Geomicrobiol Journal*, 29(6): 544–549.
- Chung, J. S., Kim, B. H., and Kim, I. S. 2014. A Case Study on Chloride Corrosion for the End Zone of Concrete Deck Subjected to De-icing Salts Added Calcium Chloride. *Journal of the Korean Society of Safety*, 29(6): 87–93.
- De Belie, N. and De Muynck, W. 2008. Crack repair in concrete using biodeposition. *Concrete Repair, Rehabilitation and Retrofitting II*, pp. 291–292.
- DeJong, J., Fritzsche, M., and Nüsslein, K. 2006. Microbially Induced Cementation to Control Sand Response to Undrained Shear. *Journal of Geotechnical and Geoenvironmental Engineering*, 132(11): 1381–1392.
- De Muynck, W., Debrouwer, D., De Belie, N., and Verstraete, W. 2008. Bacterial carbonate precipitation improves the durability of cementitious materials. *Cement and Concrete Research*, 38(7): 1005–1014.
- Dhami, N. K., M. S. Reddy, and A. Mukherjee. 2013. Biomineralization of Calcium Carbonates and Their Engineered Applications: A Review. *Frontiers in Microbiology*, 4(314): 1–13.
- Ghosh, P., Mandal, S., Chattopadhyay, B. D., and Pal, S. 2005. Use of microorganism to improve the strength of cement mortar. *Cement and Concrete Research*, 35(10): 1980–1983.
- Griffith, A. A. 1924. Theory of rupture. *Proceedings of the First International Congress on Applied Rock Mechanics*, Delft, The Netherlands, pp. 55–63.
- Harkes, M. P., van Paassen, L. A., Booster, J. L., Whiffin, V. S. and van Loosdrecht, M. C. M. 2010. Fixation and distribution of bacterial activity in sand to induce carbonate precipitation for ground reinforcement. *Ecological Engineering*, 36(2): 112–117.
- Ivanov, V., Chu, J., Stabnikov, V., He, J. and Naeimi, M. 2010. Iron based bio-grout for soil improvement and land reclamation. *Proceedings of the Second International Conference on Sustainable Construction Materials and Technologies*, Ancona, Italy, June 28–30, 2010, pp. 415–420.

- Jonkers, H. M., Thijssen, A., Muyer, G., Copuroglu, O. and Schlangen, E. 2010. Application of bacteria as self-healing agent for the development of sustainable concrete. *Ecological Engineering*, 36(2): 230–235.
- Le Metayer-Levrel, G., Castanier, S., Oriol, G., Loubiere, J.-F., and Perthuisot, J.-P. 1999. Applications of bacterial carbonatogenesis to the protection and regeneration of limestones in buildings and historic patrimony. *Sedimentary Geology*, Vol. 126, pp. 25–34.
- Li, M., Li, L., Ogbonnaya, U., Wen, K., Tian, A., and Amini, F. 2015. Influence of Fiber Addition on Mechanical Properties of MICP-Treated Sand. *Journal of Materials in Civil Engineering*, 28(4): 04015166.
- Mitchell, J. K. and Santamarina, J. C. 2005. Biological considerations in geotechnical engineering. *Journal of Geotechnical and Geoenvironmental Engineering*, 131(10): 1222–1233.
- Ng, W. S., Lee, M. S. and Hii, S. L. 2012. An Overview of the Factors Affecting Microbial-Induced Calcite Precipitation and its Potential Application in Soil Improvement. *Engineering and Technology*, World Academy of Science, 6(2): 683–689.
- Park, S., Choi, S., and Nam, I. 2014. Effect of Plant-Induced Calcite Precipitation on the Strength of Sand. *Journal of Materials in Civil Engineering*, 26(8): 06014017.
- Pei, R., Liu, J., Wang, S. and Yang, M. 2013. Use of bacterial cell walls to improve the mechanical performance of concrete. *Cement and Concrete Composites*, Vol. 39, pp. 122–130.
- Ramachandran, S. K., Ramakrishnan, V. and Bang, S. S. 2001. Remediation of concrete using micro-organisms. *ACI Materials Journal*, American Concrete Institute, Vol. 98, pp. 3–9.
- Stabnikov, V., Chu, J., Ivanov, V., and Li, Y. 2013. Halotolerant, alkaliphilic urease-producing bacteria from different climate zones and their application for biocementation of sand. *Journal of Microbiology and Biotechnology*, 29(8): 1453–1460.
- Stocks-Fisher, S. Galinat, J. K., and Bang, S. S. 1999. Microbiological precipitation of CaCO<sub>3</sub>. *Soil Biology and Biochemistry*, 31(11): 1563–1571.
- Van Paassen, L. A., Ghose, R., van der Linden, T. J. M., van der Star, W. R. L. and van Loosdrecht, M. C. M. 2010. Quantifying biomediated ground improvement by ureolysis: Large-scale biogROUT experiment. *Journal of Geotechnical and Geoenvironmental Engineering*, 136(12): 1721–1728.
- Van Tittelboom, K., De Belie, N., Muynck, W. D., and Verstraete, W. 2010. Use of bacteria to repair cracks in concrete. *Cement and Concrete Research*, Vol. 40, 157–166.
- Vempada, S. R., Reddy S. S. P., Rao, M. V. Seshagiri, and Sasikala, Ch. 2011. Strength Enhancement of Cement Mortar using Microorganisms – An Experimental Study. *International Journal of Earth Sciences and Engineering*, 04(06): 933–936.
- Wang, K., Jansen, D. C. and Shah, S. P. 1997. Permeability study of cracked concrete. *Cement and Concrete Research*, 27(3): 381–393.
- Wang, J. Y., Soens, H., Verstraete, W. and De Beie, N. 2014. Self-healing concrete by use of microencapsulated bacterial spores. *Cement and Concrete Research*, Vol. 56, pp. 139–152.
- Whiffin, V. S., van Paassen, L. A. and Harkes, M. P. 2007. Microbial Carbonate Precipitation as a Soil Improvement Technique. *Geomicrobiology Journal*, 24(5): 417–423.
- Zhang, Y., Guo, H. X., Cheng, X. H. 2014. Influences of calcium sources on microbially induced carbonate precipitation in porous media. *Materials Research Innovations*, 18(2): 79–84.

- Zhao, Q., Li, L., Li, C., Li, M., Amini, F., and Zhang, H. 2014. Factors Affecting Improvement of Engineering Properties of MICP-Treated Soil Catalyzed by Bacteria and Urease. *Journal of Materials in Civil Engineering*, 26(12): 04014094.
- Zhao, X., Chi, Z., Rover, M., Brown, R., Jarboe, L. and Wen, Z. 2013. Microalgae fermentation of acetic acid-rich pyrolytic bio-oil: Reducing bio-oil toxicity by alkali treatment. *Environmental Progress & Sustainable Energy*, 32(4): 955–961.